

RESTRICTED
Restriction/
Classification
Cancelled

Copy 5
RM SE58G01

CLASSIFICATION CANCELLED
DATE _____ BY _____

NACA RM SE58G01



Source of Acquisition
CASI Acquired

RESEARCH MEMORANDUM

for the

Air Research and Development Command, U. S. Air Force

ALTITUDE PERFORMANCE OF THE AFTERBURNER ON THE
IROQUOIS TURBOJET ENGINE

COORD. NO. AF-P-6

By Donald E. Groesbeck and Daniel J. Peters

Lewis Flight Propulsion Laboratory
Cleveland, Ohio

CLASSIFICATION CHANGE

To Unclassified
By authority of WASA Memo 522-03/4 by H. Maires
Changed by M. Ruda Date 6-6-73

Restriction/
Classification
Cancelled

This material
of the espionage
manner to unauthorized persons is prohibited by law.

DOCUMENT
National Defense of the United States within the meaning
and 704, the transmission or revelation of which in any

NATIONAL ADVISORY COMMITTEE FOR AERONAUTICS

WASHINGTON

JUL 12 8 1958

CONFIDENTIAL

CLASSIFICATION CANCELLED
 AUTHORITY: NACA TECHNICAL PUBLICATIONS
 ANNOUNCEMENTS NO. _____ DATE _____ BY _____

NATIONAL ADVISORY COMMITTEE FOR AERONAUTICS

RESEARCH MEMORANDUM

for the

Air Research and Development Command, U. S. Air Force

ALTITUDE PERFORMANCE OF THE AFTERBURNER ON THE

IROQUOIS TURBOJET ENGINE*

COORD. NO. AF-P-6

By Donald E. Groesbeck and Daniel J. Peters

The performance and operational characteristics of two afterburner configurations for the Iroquois turbojet engine were evaluated in an altitude test chamber over a range of afterburner equivalence ratios at afterburner-inlet pressures from 733 to 3186 pounds per square foot absolute. These conditions correspond to an altitude range from 38,700 to 66,800 feet at a flight Mach number of 1.5. The only difference between the two afterburner configurations was in the pattern of afterburner fuel injection.

At an afterburner-inlet pressure of approximately 3100 pounds per square foot absolute, corresponding to an altitude of 38,700 feet and a flight Mach number of 1.5, the combustion efficiency of both configurations reached peak values of 0.80 to 0.85 at equivalence ratios of 0.35 to 0.40. However, further reduction in the afterburner-inlet pressure severely affected combustion efficiency. For example, at an afterburner-inlet pressure level of 700 to 1000 pounds per square foot absolute, the efficiency for both configurations was 0.20 to 0.40.

INTRODUCTION

An investigation evaluating the performance and operational characteristics of prototype Iroquois turbojet engines was conducted in an altitude test chamber at the NACA Lewis laboratory at the request of the Air Research and Development Command, U. S. Air Force. As a part of this program, the performance and operating limits of afterburner configurations were evaluated briefly and are reported herein. Other phases of the over-all program are reported in references 1 and 2. Two afterburner configurations were evaluated. Because the performance of the first configuration (configuration A) did not meet the manufacturer's expectations, in an attempt to improve performance without making major modifications, the manufacturer provided a second configuration (configuration B) with the fuel-injection system modified to provide a somewhat altered fuel distribution and a greater mixing length.

* Title Unclassified

CLASSIFICATION CANCELLED
 AUTHORITY: NACA TECHNICAL PUBLICATIONS
 ANNOUNCEMENTS NO. _____ DATE _____ BY _____

Data were obtained over a range of afterburner equivalence ratios at afterburner-inlet total pressures from 733 to 3186 pounds per square foot absolute. These conditions correspond to altitudes from 38,700 to 66,800 feet at a flight Mach number of 1.5. The indicated afterburner-inlet total temperature was 1735° R. The performances of the two afterburner configurations are presented graphically in terms of afterburner total temperature, combustion efficiency, and pressure loss, and the two configurations are directly compared in terms of combustion efficiency, augmentation ratio, over-all specific fuel consumption, and operational limits. Tabulated afterburner performance data are presented in tables I and II.

APPARATUS

Installation

The Iroquois turbojet engine - afterburner combination installed in the altitude test chamber is shown in figure 1. A forward bulkhead (not visible in the photograph), which incorporates a labyrinth seal around the engine-inlet air duct, was used to separate the engine-inlet air from the exhaust and to provide a means of maintaining a pressure differential across the engine. A bulkhead butterfly valve was used to control the engine-inlet pressure and the amount of air used to ventilate the test chamber. Visual observation of a portion of the afterburner combustion zone was provided by a periscope located downstream of the test section and directed toward the exhaust nozzle.

Engine

The prototype twin-spool Iroquois engine used in this investigation had a nominal unaugmented sea-level static-thrust rating of 18,000 pounds with an airflow of approximately 280 pounds per second. The engine maximum low- and high-pressure rotor speeds are 5740 and 7800 rpm, respectively. The rated turbine-discharge gas temperature is 1275° F (1735° R), as indicated by an average of 25 thermocouples located at the turbine discharge.

The engine has a ten-stage two-spool axial-flow compressor; the first three stages are transonic and comprise the low-pressure compressor, an annular-type combustor, and a three-stage turbine; the last stage driving the low-pressure compressor, a diffuser assembly, an afterburner, a variable primary exhaust nozzle, and an electronic amplifier (sensing compressor-discharge and afterburner-inlet pressures) with a hydraulic control. The engine normally includes an ejector assembly; however, this assembly was inoperative for this investigation.

Two engines were used in this investigation. Engine AX 103/3A was used with afterburner configuration A and engine AX 102/3C was used with afterburner configuration B. Engine AX 103/3A is the same configuration as the "modified A" engine configuration (engine AX 103/2) of reference 1 without the friable plastic coating on the first- and second-stage compressor stator tip seals. Engine AX 102/3C is the same configuration as the "modified B" engine configuration of reference 1 except the first-stage compressor rotor blades were twisted 5° more to reduce the work at the tip of the blade. The engines are described in greater detail in reference 1.

Afterburner Configurations

The Iroquois afterburner has a nominal length of $77\frac{1}{2}$ inches and a diameter of $43\frac{1}{4}$ inches. A schematic diagram of the basic afterburner showing the location of the various components is presented in figure 2.

The afterburner discussed herein was designed for relatively low thrust augmentation, and, therefore, required operation at low over-all afterburner fuel-air ratios (equivalence ratio of approximately 0.3). It was necessary, when considering stability and efficiency, to confine the afterburner fuel flow to only a portion of the afterburner-inlet air, thus raising the local fuel-air ratio in the combustion zone. The fuel-injection system was designed in an attempt to accomplish this, and consisted of three circular rings located as shown in figure 3. Two of the injector rings were very closely coupled to the two flameholder gutters, and a third injector ring was located about 14 inches upstream of the flameholder and sized to supply fuel to the area between the two flameholder gutters. The only difference between afterburner configurations A and B was in the location and size of the fuel orifices in the fuel injector rings (fig. 3). The percentages of fuel flow from each ring remained approximately the same (as noted in fig. 3) although configuration B injected fuel in many more directions than did configuration A.

The flameholders consisted of two circular channel-like rings, each located $1/2$ inch downstream of the two downstream fuel-injector rings (fig. 3). Based on the afterburner area with a diameter of $43\frac{1}{4}$ inches, the flameholders (minus supporting rods) blocked approximately 13.7 percent of the total area.

"Hot-streak" ignition was provided for the afterburner by two fuel injectors located 120° clockwise from the top of the engine looking upstream, one immediately upstream of the turbines and the other immediately downstream. Fuel was supplied to the injectors every 4 seconds by a pulsing valve until afterburner ignition occurred.

Although no cooling liner was used in the afterburner, an antiscreech liner, 18 inches long, was installed in the plane of the downstream fuel injector rings and flameholder (fig. 2). The afterburner exhaust nozzle had a continuously variable area that ranged from approximately 649 to 1020 square inches. The afterburner control system continually adjusted the exhaust-nozzle area to maintain a maximum indicated turbine-discharge gas temperature of 1275°F (1735°R).

Looking upstream, figure 4 shows the afterburner with the flameholders, fuel rings, antiscreech liner, an afterburner ignitor, and the water-cooled total-pressure rake at the primary exhaust-nozzle inlet.

Fuel conforming to MIL-F-562a (grade JP-4) specification was used in both the engine and the afterburner. The lower heating value of the fuel was 18,700 Btu per pound and the hydrogen-carbon ratio was 0.170.

Instrumentation

The afterburner-inlet conditions were surveyed at station 6 (fig. 2) by 25 total-pressure and 25 total-temperature probes. An indicated average gas temperature of 1275°F (1735°R) was lowered to 1251°F (1711°R) by applying the thermocouple radiation and recovery corrections of references 3 and 4. The exhaust-nozzle inlet conditions (station 9) were surveyed approximately $17\frac{1}{2}$ inches upstream of the exhaust-nozzle exit with a water-cooled total-pressure rake consisting of 23 probes placed on centers of equal areas.

Standard instrumentation was provided to measure airflow, thrust, and fuel flows. Both the engine and the afterburner fuel flows were measured on remote-indicating flowmeters. A detailed description of the engine instrumentation is contained in reference 1. The symbols and method of calculation used in this report are presented in appendixes A and B, respectively. A sample calculation is presented in appendix C.

PROCEDURE

The performance characteristics of afterburner configurations A and B were obtained over a range of afterburner equivalence ratios (percent

of stoichiometric fuel-air ratio) at the following simulated flight conditions and afterburner-inlet (station 6) total pressures:

Configuration	Engine-inlet Reynolds number index	Altitude, ft	Flight Mach number, M_0	Engine-inlet total temperature, T_1 , °R	Average afterburner-inlet total pressure, P_6 , $\frac{\text{lb}}{\text{sq ft}}$ abs
A and B	0.64	38,700	1.5	566	3125
B	.51	43,200	↓	↓	2410
A and B	.37	50,400	↓	↓	1800
B	.29	54,800	↓	↓	1340
A and B	.24	59,200	↓	↓	1100
A and B	.17	66,800	↓	↓	750

In order to obtain steady-state performance data, the engine was first started and accelerated to rated speed (7800 rpm) and the engine-inlet pressure and temperature and the rated turbine-discharge gas temperature were set at the desired test conditions. The afterburner ignitors were then turned on and, upon ignition of the afterburner, the exhaust nozzle was opened by the control system. The afterburner fuel flow was set at the desired value and the exhaust-nozzle area was adjusted by the control system in order to maintain the turbine-discharge gas temperature at the rated value of 1275° F. As soon as burning was stable, the ignitors were turned off and steady-state data were taken over the operable range of afterburner equivalence ratios.

PRESENTATION OF DATA

As an aid in defining the afterburner-inlet conditions of this investigation, the calculated average afterburner-inlet velocities for the range of pressures investigated and the typical afterburner-inlet total-pressure profiles are presented in figures 5 and 6, respectively. A complete tabulation of the data, afterburning and nonafterburning, for both afterburner configurations is presented in tables I and II.

The performances of afterburner configurations A and B are presented in figure 7 for a range of afterburner-inlet pressure levels. Afterburner total temperature and combustion efficiency are presented as functions of afterburner equivalence ratio and the afterburner total-pressure-loss ratio as a function of the afterburner temperature ratio τ in figure 7.

The performances of the two afterburner configurations are compared directly in figure 8 on the basis of the variation of combustion efficiency with equivalence ratio at four afterburner-inlet pressure levels, and in figure 9 on the basis of the variation of calculated afterburner augmentation ratio and over-all specific fuel consumption with afterburner equivalence ratio for the design flight condition. The altitude operational limits of the two afterburner configurations are presented in figure 10.

RESULTS AND DISCUSSION

Average afterburner-inlet velocities of approximately 590 to 645 feet per second were encountered for both configurations over the range of afterburner-inlet pressures investigated. Peak velocities reached as high as 680 feet per second; however, these velocities are based on total-pressure measurements and could be in error to the extent of several percentage points because a flat static-pressure profile was assumed. These velocities are relatively high for good performance at altitude and are undoubtedly a contributing factor in the low efficiency levels encountered.

At the maximum afterburner-inlet pressure investigated (3100 lb/sq ft abs corresponding to an altitude of 38,700 ft at a flight Mach number of 1.5) the combustion efficiency of both configurations reached values of 0.80 to 0.85 at equivalence ratios of 0.35 to 0.40. Lowering the afterburner-inlet pressure from 3100 to 700 to 1000 pounds per square foot absolute affected the combustion efficiency very adversely. For example, at these low pressures (700 to 1000 lb/sq ft abs) the combustion efficiency for both configurations was 20 to 40 percent.

The relatively low combustion efficiencies at high altitudes are attributed to the combined effects of high afterburner-inlet velocity and short mixing length for approximately one-half the fuel that was injected through the downstream fuel rings. Injecting more of the fuel in an upstream direction in configuration B was slightly beneficial, inasmuch as the efficiency was less sensitive to inlet pressure down to approximately 1300 pounds per square foot absolute.

One problem encountered with both configurations was the inability to hold a flame stably on both gutters down to low pressures. This instability, of course, resulted in low efficiency at low pressures. Configuration B showed an improvement over configuration A in this respect.

A comparison of afterburner configurations A and B on the basis of over-all specific fuel consumption and augmentation ratio is presented in figure 9 for an altitude of 50,400 feet at a flight Mach number of 1.5. This flight condition corresponds to an engine-inlet Reynolds number

index of 0.37 and is a design point of the afterburners. Performance data shown in figure 9 were obtained by using the combustion-efficiency and pressure-loss curves of figure 7 for an afterburner-inlet total pressure of approximately 1800 pounds per square foot absolute and the computation method outlined in appendix C. This method is applicable to any altitude and Mach number combination for any of the afterburner-inlet pressures presented herein. The maximum augmentation ratio that was obtained is relatively low since the afterburners were designed for low fuel-air operation.

The lean blowout characteristics were a little better for afterburner configuration B than for configuration A. The trends of maximum equivalence ratio limits (maximum temperature as limited by maximum exhaust-nozzle area) reflect the relative combustion efficiency for the two configurations.

No troubles were encountered in igniting the afterburner down to afterburner-inlet pressures of approximately 1100 pounds per square foot absolute at fuel flows of approximately 3000 pounds per hour.

Lewis Flight Propulsion Laboratory
National Advisory Committee for Aeronautics
Cleveland, Ohio, July 7, 1958

APPENDIX A

SYMBOLS

The following symbols are used in this report:

A	area, sq ft
a	sonic velocity
B	thrust cell force, lb
C_{ve}	velocity coefficient, ratio of actual jet velocity to effective jet velocity
F	thrust, lb
F_j	unaugmented engine jet thrust, lb
$F_{j,n}$	unaugmented engine net thrust, lb
F_{AB}	augmented engine jet thrust, lb
$F_{AB,n}$	augmented engine net thrust, lb
f	fuel-air ratio
g	acceleration due to gravity, 32.17 ft/sec ²
M	Mach number
m	mass flow, slugs/sec
N	engine speed, rpm
P	total pressure, lb/sq ft abs
p	static pressure, lb/sq ft abs
R	universal gas constant, 1546 ft-lb/(lb-mole)(°R)
ReI	Reynolds number index, $P_1(T_1 + 216)/5.7738 T_1^2$
sfc	specific fuel consumption, (lb/hr)/lb
T	total temperature, °R

t	static temperature, °R
V	velocity, ft/sec
w _a	airflow, lb/sec
w _f	fuel flow, lb/sec
w _g	gas flow, lb/sec
γ	ratio of specific heats
δ ₁	ratio of engine-inlet pressure to NACA standard pressure, P/2116
η	efficiency
θ ₁	ratio of engine-inlet temperature to NACA standard temperature, T/518.7
φ	equivalence ratio
τ	afterburner temperature ratio, T _{9,AB} /T ₆

Subscripts:

AB	afterburner
ac	actual
av	average
c	calculated
corr	corrected
e	engine
eff	effective
fc	front compartment
fh	flameholder
HP	high pressure (compressor and turbine)
he	heat exchanger (bearing cooling air)
id	ideal

ind individual
LP low pressure (compressor and turbine)
N nozzle
n net
s seal
st stoichiometric
t total
0 free-stream conditions
1 engine inlet
2 low-pressure compressor outlet
3 high-pressure compressor outlet
4 engine combustor outlet (high-pressure turbine inlet)
6 low-pressure turbine outlet (afterburner inlet)
9 exhaust-nozzle inlet

APPENDIX B

METHODS OF CALCULATION

Airflow. - Airflow was determined from pressure and temperature measurements, which were used in the following equation:

$$\frac{P_A}{w_a \sqrt{(R/g)T}} = \frac{(P/p)^{1/\gamma}}{\sqrt{\frac{2\gamma}{\gamma-1} \left[1 - \left(\frac{P}{p}\right)^\gamma \right]}}$$

The right side of this equation is listed as a function of p/P in reference 5. Simple rearrangement of the equation will yield airflow.

Airflow at station 4 (engine-combustor outlet) was determined from

$$w_{a,4} = w_{a,1} - 0.68 w_{a,he} - 0.0276 w_{a,1}$$

The factors, 0.68 and 0.0276, were determined from the results of preliminary engine tests.

Airflow at station 6 (afterburner-inlet) was determined from

$$w_{a,6} = w_{a,4} + 0.0138 w_{a,1} + 0.68 w_{a,he}$$

$$w_{a,9} = w_{a,6}$$

Gas flow. - Gas flow was obtained by adding fuel flow to the airflow at the station; that is,

$$w_{g,9} = w_{a,9} + w_{f,e(\text{nonafterburning})}$$

$$w_{g,9} = w_{a,9} + w_{f,e} + w_{f,AB(\text{afterburning})}$$

$$w_{g,6} = w_{a,6} + w_{f,e}$$

Equivalence ratio. - Equivalence ratios were determined as follows:

$$\phi = f/f_{st}$$

For the fuel used in this investigation

$$f_{st} = 0.0676$$

CONFIDENTIAL

Therefore,

$$\phi_e = \frac{w_{f,e}/w_{a,4}}{0.0676}$$

$$\phi_{AB} = \frac{w_{f,AB}/w_{a,6}}{0.0676}$$

and

$$\phi_{t,ac} = \phi_e + \phi_{AB}$$

where $\phi_{t,ac}$ is the actual equivalence ratio based on total fuel flow.

The equivalence ratio based on unburned air was determined from the equation

$$\phi_{AB,ac} = \frac{\phi_{t,ac} - \phi_{e,id}}{1 - \phi_{e,id}}$$

where $\phi_{e,id}$ is the ideal equivalence ratio for the temperature rise from engine-inlet to afterburner-inlet stations (shown in table I in ref. 6).

The ideal equivalence ratio $\phi_{t,id}$ is determined from the temperature rise from the engine-inlet to the exhaust-nozzle exit (shown in table I in ref. 6). The ideal equivalence ratio for the afterburner based on unburned air was determined from the equation

$$\phi_{AB,id} = \frac{\phi_{t,id} - \phi_{e,id}}{1 - \phi_{e,id}}$$

Combustion efficiency. - Combustion efficiency was then determined from

$$\eta_{AB} = \frac{\phi_{AB,id}}{\phi_{AB,ac}}$$

Jet thrust. - Scale jet thrust was determined from the facility thrust cell and the pressure force across the seal area, A_s

$$F = B + A_s (P_{fc} - P_{tank})$$

Velocity coefficient. - Velocity coefficient was determined from non-afterburning data as follows:

$$C_{ve} = \frac{F_j}{F_{j,c}} = \frac{B + A_s (P_{fc} - P_{\text{tank}})}{w_{g,9} \frac{V_{\text{eff}}}{gRT_9} \sqrt{\frac{R}{g}} \sqrt{T_9}} \quad (\text{nonafterburning})$$

where $C_{ve} = 0.975$ for the range of data obtained, and $V_{\text{eff}}/\sqrt{gRT}$ is an effective velocity parameter and is a function of (P_{tank}/P_9) and γ_9 (ref. 5).

Gas temperature. - Afterburner total temperature was calculated as follows:

$$T_{9,AB} = \left[\frac{F_{AB}/C_{ve}}{w_{g,9} \sqrt{\frac{R}{g}} \left(\frac{V_{\text{eff}}}{\sqrt{gRT}} \right)} \right]^2$$

Afterburner-inlet velocity. - Afterburner-inlet velocity (nonafterburning) was determined from the measured quantities $w_{g,6}$, T_6 , P_6 , and A_{fh} and the following equation, assuming an area coefficient of 0.9 for the flow passage:

$$\frac{w_{g,9} \sqrt{T_6}}{A_{fh} P_6} \sqrt{\frac{R}{g}} = \frac{M_6}{\left(1 + \frac{\gamma - 1}{2} M_6^2 \right)^{\frac{\gamma+1}{2(\gamma-1)}}}$$

where

$$A_{fh} = 0.9 (9.85 \text{ sq ft}) = 8.865 \text{ sq ft}$$

The right side of this equation is listed in reference 7, and $\gamma = 1.33$ should be used to determine the Mach number at the afterburner-inlet. Static-to-total temperature ratio t/T is a function of the Mach number M ; therefore,

$$t_6 = (t/T) T_6$$

Sonic velocity, a_6 , equals $\sqrt{\gamma_6 g R t_6}$ ($\gamma_6 = 1.33$) and

$$V_6 \text{ (in ft/sec)} = M_6 a_6$$

Net thrust. - Net thrust was calculated from the following equation:

$$F_{AB,n} = F_{AB} - (w_{a,1}/g) V_1$$

where V_1 is determined from (V/\sqrt{gRT}) in reference 5 and is a function of p_{tank}/P_1 and γ_1 .

APPENDIX C

SAMPLE CALCULATION

A Reynolds number index of 0.37 could correspond to the following altitudes and Mach numbers:

Altitude, ft	Mach number
40,200	0.9
50,400	1.5
60,400	2.0

Selecting the flight condition of a 50,400-foot altitude and a Mach number of 1.5 for a sample calculation yields

$$p_0 = 238 \text{ lb/sq ft abs}$$

$$P_1 = 874 \text{ lb/sq ft abs}$$

$$T_1 = 566^\circ \text{ R}$$

At rated engine conditions (for the AX 102/3C engine),

$$N_{HP} = 7800 \text{ rpm or } N_{HP}/\sqrt{\theta_1} = 7464 \text{ rpm}$$

$$T_{6,corr} = 1711^\circ \text{ R or } T_6/T_1 = 3.03$$

From an over-all engine performance map, the intersection of $N_{HP} = 7464 \text{ rpm}$ and $T_6/T_1 = 3.03$ gives $w_{a,1}\sqrt{\theta_1}/\delta_1 = 258.8$ pounds per second and $P_6/P_1 = 2.06$ (ref. 1), where

$$P_6 = (P_6/P_1)P_1 = 1803 \text{ lb/sq ft abs}$$

$$w_{a,1} = (w_{a,1}\sqrt{\theta_1}/\delta_1)(\delta_1/\sqrt{\theta_1}) = 102.3 \text{ lb/sec}$$

A mechanical engine speed limit for N_{LP} of 5740 rpm should not be exceeded for the particular flight condition under consideration (altitude, 50,400 ft; Mach number, 1.5); in this instance, $N_{LP} = 5739 \text{ rpm}$.

Nonafterburning conditions. - At an afterburner temperature ratio of 1.0 and a Reynolds number index of 0.37 (from fig. 7(b))

$$(P_6 - P_9)/P_6 = 0.07 \quad \text{or} \quad P_9 = 1677 \text{ lb/sq ft abs}$$

From reference 6, the ideal engine equivalence ratio $\phi_{e,id}$ is 0.240. Defining $\eta_e = \phi_{e,id}/\phi_{e,ac}$ and assuming $\eta_e = 0.98$ yields

$$\phi_{e,ac} = 0.245$$

Since $\phi_{e,ac} = (w_{f,e}/w_{a,1})/f_{st}$ then,

$$w_{f,e} = 1.70 \text{ lb/sec}$$

If the air lost overboard through acceleration bleeds, air turbine pumps, and so forth is assumed to equal $w_{f,e}$, then $w_{g,9} = w_{a,1} = 102.3$ pounds per second.

With the appropriate γ_9 , reference 5 gives $V_{eff}/\sqrt{gRT} = 1.660$ and $F_j = C_{ve} m_9 V_{eff} = 8820$ pounds when $C_{ve} = 0.975$.

At a 50,400-foot altitude, the speed of sound is 968.5 feet per second, or at a Mach number of 1.5, the velocity V_0 is $1.5(968.5)$ or 1453 feet per second.

The inlet momentum term mV_0 is

$$mV_0 = (102.3/32.17)1453 = 4621 \text{ lb}$$

or

$$F_{j,n} = F_j - mV_0 = 4199 \text{ lb}$$

Afterburning conditions. - From figure 7(b), at $\phi_{AB,ac} = 0.4$ and a Reynolds number index of 0.37,

$$\eta_{AB} = 0.68$$

and

$$T_{9,AB} = 2525^{\circ} \text{ R}$$

From figure 7(b) at $\tau = T_{9,AB}/T_6 = 2525/1711 = 1.48$,

$$(P_6 - P_9)/P_6 = 0.091 \quad \text{or} \quad P_9 = 1639 \text{ lb/sq ft abs}$$

$$\text{From } \phi_{AB,ac} = \frac{\phi_{t,ac} - \phi_{e,id}}{1 - \phi_{e,id}}$$

$$\phi_{t,ac} = 0.544 = \phi_{AB} + \phi_{e,ac}$$

or

$$\phi_{AB} = 0.299 = (w_{f,AB}/w_{a,6})/f_{st}$$

If the air lost overboard is assumed equal to $w_{f,e}$,

$$w_{a,6} = w_{a,1} - w_{f,e}$$

Therefore,

$$w_{a,6} = 100.6 \text{ lb/sec and } w_{f,AB} = 2.03 \text{ lb/sec}$$

$$w_{g,6} = w_{a,6} + w_{f,e}$$

$$w_{g,9} = w_{g,6} + w_{f,AB} = 104.3 \text{ lb/sec}$$

Since

$$\phi_{AB,id} = \eta_{AB}(\phi_{AB,ac}) = 0.272 = \frac{\phi_{t,id} - \phi_{e,id}}{1 - \phi_{e,id}}$$

$$\phi_{t,id} = 0.447$$

and from reference 6,

$$T_{9,AB} - T_1 = 1975^\circ \text{ R or } T_{9,AB} = 2541^\circ \text{ R}$$

At $\gamma_9 = 1.288$

$$(V_{eff}/\sqrt{gRT})_9 = 1.665 \text{ (ref. 5)}$$

For $C_{ve} = 0.975$

$$F_{AB} = C_{ve} m_9 V_{eff} = 10,993 \text{ lb}$$

Since $mV_0 = 4621$ pounds,

$$F_{AB,n} = 10,993 - 4621 = 6372 \text{ lb}$$

The net augmented thrust ratio is then 1.518, the afterburner temperature rise τ is 1.485, and the over-all specific fuel consumption sfc is $\frac{w_{f,AB} + w_{f,e}}{F_{AB,n}}$ or 2.11. Using the previous method, other values of $\phi_{AB,ac}$, altitudes, and Mach numbers can be used to give complete curves as shown in figure 9.

REFERENCES

1. McAulay, John E., and Groesbeck, Donald E.: Investigation of a Prototype Iroquois Turbojet Engine in an Altitude Test Chamber. NACA RM SE58E26, 1958.
2. Peters, Daniel J., and McAulay, John E.: Some Altitude Operational Characteristics of a Prototype Iroquois Turbojet Engine. NACA RM SE58F17, 1958.
3. Glawe, George W., Simmons, Frederick S., and Stickney, Truman M.: Radiation and Recovery Corrections and Time Constants of Several Chromel-Alumel Thermocouple Probes in High-Temperature, High-Velocity Gas Streams. NACA TN 3766, 1956.
4. Scadron, Marvin D., and Warshawsky, Isidore: Experimental Determination of Time Constants and Nusselt Numbers for Bare-Wire Thermocouples in High-Velocity Air Streams and Analytic Approximation of Conduction and Radiation Errors. NACA TN 2599, 1952.
5. Turner, L. Richard, Addie, Albert N., and Zimmerman, Richard H.: Charts for the Analysis of One-Dimensional Steady Compressible Flow. NACA TN 1419, 1948.
6. Huntley, S. C.: Ideal Temperature Rise Due to a Constant-Pressure Combustion of a JP-4 Fuel. NACA RM E55G27a, 1955.
7. Lewis Laboratory Computing Staff: Tables of Various Mach Number Functions for Specific-Heat Ratios from 1.28 to 1.38. NACA TN 3981, 1957.

TABLE I. - PERFORMANCE OF AFTERBURNER CONFIGURATION A

(a) Afterburning data

Run	Engine-inlet Reynolds number index, ReI	High-pressure compressor rotor speed, N_{HP} , rpm	Low-pressure compressor rotor speed, N_{LP} , rpm	Engine-inlet total temperature, T_1 , $^{\circ}R$	Engine-inlet total pressure, P_1 , lb/sq ft abs	High-pressure compressor-inlet total temperature, T_2 , $^{\circ}R$	High-pressure compressor-inlet total pressure, P_2 , lb/sq ft abs	High-pressure compressor-outlet total temperature, T_3 , $^{\circ}R$	High-pressure compressor-outlet total pressure, P_3 , lb/sq ft abs	High-pressure turbine-inlet total pressure, P_4 , lb/sq ft abs	Low-pressure turbine-outlet total temperature, T_6 , $^{\circ}R$	Low-pressure turbine-outlet total pressure, P_6 , lb/sq ft abs	Exhaust nozzle-inlet total pressure, P_9 , lb/sq ft abs	Tank static pressure, P_{tank} , lb/sq ft abs
1	0.653	7755	5103	569	1556	673	2678	1059	9,947	9120	1659	3156	2895	371
2	.635	7810	5150	564	1494	676	2625	1065	9,814	9016	1667	3085	2811	359
3	.640	7778	5126	564	1508	670	2583	1059	9,856	9035	1674	3112	2893	364
4	.633	7790	5171	564	1490	672	2595	1059	9,848	9032	1675	3107	2895	360
5	.650	7785	5122	569	1548	667	2667	1066	9,954	9134	1674	3145	2932	397
6	.648	7806	5116	571	1549	678	2682	1067	10,049	9221	1687	3186	2973	367
7	.646	7750	4912	571	1545	673	2639	1058	9,824	9019	1690	3179	2971	403
8	.648	7799	5143	571	1549	680	2676	1069	10,019	9233	1681	3134	2942	400
9	.368	7809	5276	565	868	682	1592	1075	5,903	5434	1678	1809	1613	221
10	.375	7797	5377	560	875	679	1580	1069	5,915	5422	1665	1775	1584	234
11	.374	7783	5279	560	873	676	1553	1068	5,873	5402	1672	1789	1624	264
12	.373	7778	5265	562	874	675	1564	1065	5,875	5399	1677	1811	1649	249
13	.377	7810	5269	561	882	676	1571	1071	6,027	5563	1712	1873	1746	234
14	.371	7787	5338	562	869	680	1557	1071	5,788	5302	1659	1756	1624	244
15	.372	7780	5170	562	872	673	1528	1065	5,827	5359	1710	1826	1699	237
16	.369	7747	5170	564	869	673	1519	1064	5,753	5280	1690	1790	1666	241
17	.245	7676	5109	564	576	670	1000	1057	3,710	3406	1675	1129	1023	157
18	.241	7756	5320	565	569	682	1010	1072	3,710	3406	1673	1121	1017	198
19	.244	7712	5196	564	574	675	1015	1067	3,723	3416	1665	1123	1023	160
20	.242	7735	5220	565	571	678	1006	1066	3,724	3420	1678	1133	1040	203
21	.243	7736	5146	564	572	673	1005	1068	3,721	3412	1673	1116	1026	163
22	.244	7740	5330	565	575	682	1018	1073	3,736	3428	1666	1128	1037	162
23	.240	7750	5300	564	566	680	1006	1069	3,713	3405	1673	1120	1033	213
24	.244	7724	5219	563	573	675	1003	1062	3,724	3419	1678	1139	1055	215
25	^a .166	7786	5457	571	398	695	707	1089	2,528	2315	1675	747	676	210
26	^a .167	7776	5450	571	399	695	707	1089	2,523	2312	1660	749	678	201
27	^a .167	7780	5404	572	401	695	702	1089	2,471	2260	1699	733	665	182
28	^a .165	7773	5451	574	398	698	705	1089	2,478	2269	1668	735	667	184

^aQuestionable combustion stability.

TABLE I. - Continued. PERFORMANCE OF AFTERBURNER CONFIGURATION A

(a) Concluded. Afterburning data

Engine-inlet air-flow, $w_{a,1}$, lb/sec	High-pressure turbine-inlet airflow, $w_{a,4}$, lb/sec	Exhaust-nozzle inlet airflow, $w_{a,9}$, lb/sec	Engine fuel flow, $w_{f,e}$, lb/hr	After-burner fuel flow, $w_{f,AB}$, lb/hr	Exhaust-nozzle inlet gas flow, $w_{g,9}$, lb/sec	After-burner equivalence ratio, $\phi_{AB,ac}$	Aug-mented jet thrust, F_{AB} , lb	Aug-mented net thrust, $F_{AB,n}$, lb	Calcu-lated after-burner total temper-ature, $T_{9,AB}$, $^{\circ}R$	Exhaust-nozzle area, A_N , sq in.	After-burner effi-ciency, η_{AB}	Tailpipe total-pressure loss, $\frac{P_6 - P_9}{P_6}$	After-burner total-temper-ature ratio, τ , $\frac{T_{9,AB}}{T_6}$	Run
177.92	172.01	175.47	9691	11,768	181.43	0.360	19,671	11,458	2607	954	0.853	0.083	1.571	1
175.34	167.14	172.92	9594	10,652	178.54	.336	19,125	11,082	2544	931	.842	.089	1.526	2
174.99	166.66	172.57	9634	9,122	177.78	.239	18,597	10,577	2421	890	.830	.070	1.446	3
173.70	165.29	171.30	9677	6,862	175.89	.225	17,836	9,877	2274	847	.840	.068	1.358	4
177.12	170.12	174.67	9691	5,648	178.93	.176	17,537	9,502	2171	820	.881	.068	1.283	5
178.10	171.92	175.65	9857	5,213	179.84	.162	17,494	9,246	2096	811	.790	.067	1.242	6
175.10	168.23	172.68	9778	4,381	176.61	.141	16,784	8,860	2043	768	.773	.066	1.209	7
176.84	169.83	174.40	9752	3,532	178.09	.112	16,581	8,557	1966	773	.774	.061	1.170	8
105.38	100.99	103.93	5886	12,319	108.99	.642	11,939	7,168	2696	1006	.523	.108	1.607	9
104.30	100.10	102.86	5728	11,171	107.55	.585	11,337	6,694	2547	996	.487	.108	1.530	10
103.67	99.52	102.24	5767	9,792	106.56	.519	10,984	6,531	2505	958	.516	.092	1.498	11
104.04	99.97	102.60	5782	8,291	106.51	.438	10,660	6,099	2316	907	.463	.090	1.381	12
105.79	101.39	104.33	6116	7,812	108.20	.401	10,701	5,977	2197	841	.384	.073	1.283	13
102.58	98.43	101.16	5638	6,955	104.66	.373	9,967	5,453	2101	855	.365	.075	1.266	14
101.91	97.83	100.50	5832	5,447	103.63	.298	9,719	5,197	2003	790	.305	.070	1.171	15
101.15	97.11	99.75	5699	3,884	102.41	.215	9,130	4,654	1832	755	.198	.069	1.084	16
64.87	62.18	63.97	3643	8,060	67.23	.686	7,175	4,292	2633	975	.458	.094	1.572	17
65.52	62.82	64.62	3640	7,297	67.66	.611	6,670	3,977	2433	968	.399	.093	1.454	18
65.57	62.86	64.67	3614	6,901	67.59	.576	6,795	3,898	2357	929	.382	.089	1.416	19
65.13	62.85	64.23	3668	5,846	66.88	.496	6,429	3,775	2318	909	.411	.082	1.381	20
65.14	62.44	64.24	3632	5,432	66.76	.460	6,440	3,579	2184	870	.348	.080	1.305	21
65.85	63.13	64.94	3650	4,050	67.08	.342	6,122	3,222	1955	829	.255	.081	1.173	22
65.00	62.30	64.10	3654	3,434	66.07	.297	5,731	3,145	1936	802	.268	.077	1.157	23
65.45	62.75	64.55	3668	2,538	66.28	.219	5,530	2,924	1791	761	.155	.074	1.067	24
43.98	41.37	43.37	2470	6,012	45.73	.753	3,880	2,415	2271	899	.250	.096	1.356	25
43.93	41.32	43.32	2455	5,962	45.66	.747	3,920	2,411	2256	917	.249	.095	1.359	26
43.13	42.08	42.54	2376	5,162	44.63	.652	3,879	2,297	2207	955	.247	.093	1.299	27
43.17	42.15	42.57	2416	4,021	44.36	.517	3,787	2,218	2144	955	.284	.094	1.285	28

CONFIDENTIAL

NACA RM SFS8301

CONFIDENTIAL

TABLE I. - Continued. PERFORMANCE OF AFTERBURNER CONFIGURATION A

(b) Nonafterburning data

Run	Engine-inlet Reynolds number index, ReI	High-pressure compressor rotor speed, N_{HP} , rpm	Low-pressure compressor rotor speed, N_{LP} , rpm	Engine-inlet total temperature, T_1 , $^{\circ}R$	Engine-inlet total pressure, P_1 , lb/sq ft abs	High-pressure compressor-inlet total temperature, T_2 , $^{\circ}R$	High-pressure compressor-inlet total pressure, P_2 , lb/sq ft abs	High-pressure compressor-outlet total temperature, T_3 , $^{\circ}R$	High-pressure compressor-outlet total pressure, P_3 , lb/sq ft abs	High-pressure turbine-inlet total pressure, P_4 , lb/sq ft abs	Low-pressure turbine-outlet total pressure, P_6 , lb/sq ft abs	Exhaust nozzle-inlet total temperature, T_9 , $^{\circ}R$	Exhaust nozzle-inlet total pressure, P_9 , lb/sq ft abs	Tank static pressure, P_{tank} , lb/sq ft abs
1	0.652	7762	5085	566	1543	645	2658	1057	10,064	9246	3230	1689	3049	371
2	.655	7780	5245	565	1492	665	2628	1061	9,948	9136	3137	1672	2945	367
3	.540	6920	5255	441	925	560	1787	855	5,881	5354	1533	1167	1103	372
4	.553	7098	5434	454	891	562	1813	876	6,283	5712	1643	1242	1184	497
5	.532	7010	5322	440	907	561	1777	867	6,040	5494	1618	1220	1352	362
6	.532	7035	5327	440	906	562	1795	870	6,035	5492	1587	1217	1287	229
7	.531	7026	5317	440	905	561	1788	869	6,082	5530	1593	1222	1312	314
8	.530	7103	5444	436	892	561	1811	878	6,237	5688	1639	1247	1183	452
9	.527	7045	5395	440	899	563	1791	874	6,061	5526	1590	1225	1141	394
10	.527	7047	5337	441	901	563	1789	870	6,061	5521	1592	1223	1313	395
11	.516	7040	5371	441	881	564	1764	874	6,004	5466	1560	1217	1126	221
12	.503	7676	5221	440	858	543	1601	936	7,182	6668	2362	1717	2229	496
13	.492	7614	5218	447	856	550	1607	934	7,042	6533	2244	1648	2115	406
14	.491	7619	5206	447	855	549	1601	933	7,031	6506	2238	1645	2110	220
15	.487	7646	5235	448	850	553	1603	938	7,021	6491	2237	1650	2116	311
16	.462	7293	5166	411	718	519	1384	858	5,878	5434	1807	1463	1683	425
17	.458	6734	4520	423	741	503	1316	790	4,905	4492	1472	1219	1382	419
18	.443	7010	4950	419	708	519	1336	816	5,286	4858	1595	1313	1489	413
19	.432	6472	4358	432	719	509	1197	779	3,983	3618	1186	1129	1104	418
20	.431	7585	5090	510	892	614	1592	991	6,357	5869	2006	1620	1883	241
21	.430	7604	5057	510	889	613	1590	992	6,416	5889	2027	1635	1911	222
22	.428	7590	5049	513	893	616	1598	994	6,360	5862	2010	1617	1879	293
23	.426	7605	5055	515	893	619	1596	997	6,371	5833	2007	1622	1886	362
24	.423	7584	5040	521	898	624	1583	1001	6,289	5795	1991	1622	1871	455
25	.420	7612	5065	518	888	621	1583	1001	6,338	5856	2007	1640	1881	409
26	.419	7602	5020	523	896	626	1585	1002	6,270	5774	1996	1647	1877	506
27	.412	7420	4810	504	840	595	1425	947	5,432	4995	1768	1559	1688	467
28	.404	7700	5133	503	821	614	1519	999	6,085	5630	1904	1615	1799	503
29	.393	7822	5565	498	788	623	1527	1017	6,272	5774	1889	1680	1758	459
30	.392	7183	4521	504	799	587	1306	927	4,842	4462	1617	1516	1535	484
31	.391	6944	4345	504	797	580	1259	897	4,367	4010	1448	1415	1375	486
32	.390	6670	4148	502	791	574	1208	863	3,883	3539	1278	1294	1214	473
33	.389	5467	3066	510	804	549	1017	730	2,219	1959	771	902	739	487
34	.388	6373	3907	506	795	568	1156	831	3,410	3064	1108	1177	1053	476
35	.383	6039	3620	509	790	562	1091	790	2,870	2555	934	1041	887	468
36	.381	7740	5130	564	897	669	1558	1053	5,956	5492	1891	1696	1774	243
37	.377	7784	5263	564	889	679	1597	1071	5,984	5518	1849	1685	1727	237
38	.376	7603	5510	565	886	695	1600	1055	5,319	4848	1471	1487	1330	514
39	.376	7580	5530	564	885	693	1596	1052	5,279	4806	1464	1477	1320	412
40	.375	7615	5538	564	882	695	1590	1056	5,307	4833	1467	1490	1330	451
41	.373	7786	5296	560	871	673	1566	1066	6,054	5579	1877	1707	1753	240
42	.370	7780	5211	565	873	675	1541	1064	5,911	5451	1858	1705	1740	251
43	.370	7600	5543	563	870	694	1568	1055	5,222	4749	1442	1482	1299	351
44	.369	7760	5188	569	878	680	1535	1070	5,753	5268	1788	1685	1667	236
45	.368	7580	5519	562	862	693	1554	1051	5,147	4685	1420	1476	1282	241
46	.367	7776	5206	569	874	680	1533	1070	5,778	5294	1786	1681	1675	230
47	.367	7820	5336	561	858	678	1559	1072	5,993	5525	1835	1688	1714	243
48	.358	7643	5554	563	842	694	1519	1057	5,116	4667	1422	1492	1287	298
49	.245	7717	5153	562	574	672	998	1062	3,708	3412	1154	1693	1080	216
50	.243	7750	5324	565	573	683	1005	1070	3,735	3428	1139	1678	1062	189
51	.176	6610	4764	499	354	569	538	855	1,685	1533	550	1300	519	198
52	.175	6295	3913	500	353	563	508	818	1,457	1308	469	1170	441	206
53	.173	6960	4429	497	346	577	551	901	1,899	1737	627	1468	592	221
54	.167	7750	5478	566	394	691	701	1082	2,488	2280	737	1658	679	192
55	.149	7733	5518	562	349	691	627	1077	2,207	2020	642	1639	587	168

^aUnchoked exhaust nozzle.

^bCooling air on; measured thrust questionable.

TABLE I. - Concluded. PERFORMANCE OF AFTERBURNER CONFIGURATION A

(b) Concluded. Nonafterburning data

Engine-inlet air-flow, $w_{a,1}$, lb/sec	High-pressure turbine-inlet airflow, $w_{a,4}$, lb/sec	Exhaust-nozzle inlet airflow, $w_{a,9}$, lb/sec	Engine-fuel flow, $w_{f,e}$, lb/hr	Exhaust-nozzle inlet gas flow, $w_{g,9}$, lb/sec	Unaugmented jet thrust, F_J , lb	Unaugmented net thrust, $F_{J,N}$, lb	Calculated engine jet thrust, F_J , lb	Exhaust-nozzle velocity coefficient, C_{ve}	Exhaust-nozzle area, A_N , sq in.	Tailpipe total-pressure loss, $\frac{P_6 - P_9}{P_6}$	Run
178.34	170.43	175.88	9954	178.65	15,590	9464	15,980	0.976	701	0.056	1
175.72	166.94	173.29	9756	176.00	15,373	8947	15,626	.984	717	.061	2
120.62	116.08	118.95	4266	120.14	6,974	2856	7,208	.968	1009	.280	3
125.72	121.70	123.99	4910	125.35	6,840	3342	7,075	.967	1009	.279	4
122.38	117.69	120.69	4594	121.97	7,796	3605	8,048	.969	896	.164	5
122.37	117.69	120.68	4565	121.95	8,549	3652	8,760	.976	899	.189	6
122.46	117.77	120.77	4594	122.05	8,061	3616	8,289	.972	888	.176	7
125.27	120.87	123.55	4892	124.91	7,108	3364	7,384	.963	1009	.278	8
122.70	118.01	121.01	4622	122.29	7,191	3177	7,458	.964	1009	.282	9
122.30	117.62	120.61	4615	121.89	7,604	3598	7,788	.976	892	.175	10
120.48	116.13	118.82	4579	120.09	8,112	3278	8,478	.957	1009	.278	11
129.36	124.64	127.58	7967	129.79	10,294	6775	10,672	.965	701	.056	12
127.57	122.56	125.81	7531	127.90	10,350	6329	10,599	.977	701	.057	13
127.96	122.95	126.19	7538	128.28	11,172	6033	11,494	.972	700	.057	14
127.16	122.17	125.41	7542	127.51	10,698	6155	11,018	.971	703	.054	15
113.09	109.35	111.52	5713	113.11	7,963	5048	8,319	.957	721	.066	16
100.86	97.70	99.47	3942	100.56	6,165	3427	6,397	.964	721	.061	17
104.57	100.81	103.12	4612	104.40	6,875	4123	7,085	.970	721	.066	18
84.95	81.71	83.78	2801	84.55	4,605	2325	4,768	.966	716	.069	19
114.29	109.67	112.72	6343	114.48	9,822	4982	9,817	.986	701	.061	20
115.05	110.40	113.46	6448	115.25	9,973	5001	10,041	.979	968	.057	21
114.47	109.84	112.89	6350	114.65	9,571	4989	9,586	.984	700	.065	22
114.45	109.83	112.87	6365	114.64	9,246	5037	9,287	.981	699	.060	23
112.23	107.69	110.68	6214	112.41	8,584	4916	8,672	.975	700	.060	24
113.02	108.42	111.46	6350	113.22	8,981	5079	8,998	.983	699	.063	25
111.95	107.59	110.41	6235	112.14	8,339	4952	8,491	.968	698	.060	26
99.55	95.70	98.17	5195	99.62	7,192	4201	7,389	.973	663	.045	27
109.26	105.86	107.75	6214	109.48	8,053	5035	8,243	.977	709	.055	28
110.18	106.29	108.66	6415	110.44	8,285	5354	8,646	.958	731	.069	29
90.15	86.37	88.91	4536	90.17	6,153	3635	6,331	.972	655	.052	30
83.84	80.41	82.69	3776	83.73	5,333	3002	5,450	.979	655	.051	31
78.02	74.93	76.94	3020	77.78	4,485	2384	4,639	.967	655	.050	32
52.42	50.21	51.69	972	51.96	1,749	275	1,815	.963	655	.041	33
69.98	67.09	69.02	2293	69.65	3,588	1606	3,678	.975	655	.050	34
61.90	59.39	61.05	1627	61.50	2,700	925	2,768	.975	655	.050	35
104.42	100.15	102.98	5432	104.65	9,079	4431	9,253	.981	694	.062	36
106.83	102.45	105.36	5944	107.01	9,041	4266	9,426	.959	723	.066	37
97.33	93.40	95.99	4475	97.23	6,085	3093	6,252	.973	790	.096	38
97.03	93.11	95.69	4428	96.92	6,536	3058	6,740	.970	790	.098	39
96.55	92.64	95.22	4482	96.46	6,416	3153	6,545	.980	790	.093	40
105.79	101.47	104.33	6156	106.04	9,198	4527	9,413	.977	710	.066	41
102.78	98.65	101.36	5989	103.03	8,941	4392	9,117	.981	703	.064	42
95.14	91.26	93.82	4410	95.05	6,825	3155	6,914	.987	790	.099	43
100.74	96.93	99.35	9263	100.92	8,594	4080	8,858	.970	717	.068	44
94.52	90.69	93.22	4316	94.41	7,263	3100	7,421	.979	790	.097	45
101.17	97.23	99.78	5692	101.36	8,717	4157	8,920	.977	713	.062	46
104.75	100.37	103.30	6048	104.98	9,052	4457	9,223	.982	738	.066	47
92.66	88.84	91.39	4416	92.61	6,952	3172	7,021	.990	790	.095	48
65.19	62.48	64.29	3701	65.32	5,328	2736	5,448	.978	712	.064	49
65.46	62.79	64.55	3690	65.56	5,376	2633	5,554	.968	734	.068	50
33.25	31.87	32.79	1328	33.16	1,925	937	2,000	.962	655	.057	51
30.02	28.55	29.61	1004	29.88	1,496	632	1,547	.967	655	.059	52
36.16	34.71	35.66	1728	36.14	2,254	1302	2,343	.962	655	.055	53
43.71	41.88	43.10	2412	43.77	3,238	1710	3,332	.972	759	.079	54
38.61	36.99	38.08	2009	38.77	2,796	1444	2,911	.961	763	.086	55

^aCooling air on; measured thrust questionable.

TABLE II. - PERFORMANCE OF AFTERBURNER CONFIGURATION B

(a) Afterburning data

Run	Engine-inlet Reynolds number index, ReI	High-pressure compressor rotor speed, N_{HP} , rpm	Low-pressure compressor rotor speed, N_{LP} , rpm	Engine-inlet total temperature, T_1 , °R	Engine-inlet total pressure, P_1 , lb/sq ft abs	High-pressure compressor-inlet total temperature, T_2 , °R	High-pressure compressor-inlet total pressure, P_2 , lb/sq ft abs	High-pressure compressor-outlet total temperature, T_3 , °R	High-pressure compressor-outlet total pressure, P_3 , lb/sq ft abs	High-pressure turbine-inlet total pressure, P_4 , lb/sq ft abs	Low-pressure turbine-outlet total temperature, T_6 , °R	Low-pressure turbine-outlet total pressure, P_6 , lb/sq ft abs	Exhaust nozzle-inlet total pressure, P_9 , lb/sq ft abs	Tank static pressure, P_{tank} , lb/sq ft abs
1	0.639	7810	5460	571	1527	694	2860	1082	10,399	9448	1672	3079	2740	408
2	.641	7786	5348	570	1530	688	2824	1077	10,329	9372	1690	3120	2805	393
3	.640	7812	5486	570	1528	695	2847	1085	10,314	9364	1668	3064	2773	400
4	.635	7808	5412	574	1529	694	2820	1083	10,217	9291	1684	3076	2811	395
5	.648	7790	5422	569	1542	691	2867	1079	10,419	9453	1671	3112	2854	407
6	.509	7800	5450	576	1231	701	2271	1090	8,200	7468	1663	2451	2190	417
7	.504	7782	5406	583	1237	705	2251	1093	7,952	7253	1705	2363	2111	429
8	.503	7788	5456	583	1236	708	2272	1095	7,992	7258	1661	2339	2088	452
9	.514	7818	5449	571	1229	694	2288	1086	8,331	7584	1688	2481	2258	421
10	.508	7803	5463	578	1234	702	2280	1092	8,182	7450	1673	2403	2204	456
11	.515	7788	5391	571	1233	692	2273	1082	8,268	7538	1687	2485	2301	436
12	.517	7787	5405	571	1236	693	2277	1084	8,251	7515	1685	2473	2291	444
13	.516	7794	5393	573	1241	694	2284	1085	8,242	7499	1685	2474	2297	446
14	.364	7788	5454	573	874	695	1613	1086	5,821	5312	1689	1758	1559	220
15	.361	7793	5416	574	870	696	1602	1086	5,808	5307	1700	1744	1588	253
16	.364	7777	5358	573	875	693	1597	1082	5,815	5307	1700	1751	1607	246
17	.359	7817	5445	574	865	698	1603	1089	5,792	5289	1695	1724	1585	242
18	.364	7783	5435	574	876	692	1597	1083	5,813	5305	1703	1753	1627	242
19	.294	7814	5631	573	706	704	1317	1099	4,660	4234	1665	1348	1211	374
20	.293	7823	5600	571	702	702	1315	1100	4,680	4263	1670	1352	1230	380
21	.294	7796	5615	571	704	703	1325	1093	4,643	4215	1652	1326	1206	378
22	.297	7798	5585	569	707	699	1328	1091	4,696	4275	1663	1348	1228	379
23	.297	7794	5583	569	707	699	1323	1088	4,691	4258	1661	1352	1239	380
a24	.240	7784	5546	570	572	699	1061	1086	3,742	3398	1670	1084	967	177
a25	.241	7780	5525	570	574	696	1066	1085	3,766	3434	1683	1098	978	154
a26	.239	7789	5541	571	571	698	1062	1089	3,750	3412	1684	1088	980	182
b27	.239	7807	5497	570	570	694	1066	1088	3,793	3459	1726	1116	1008	157
a28	.240	7787	5525	569	572	696	1064	1087	3,776	3446	1681	1099	998	180
a29	.241	7794	5505	569	573	706	1081	1093	3,748	3400	1655	1058	954	184
a30	.239	7796	5537	571	572	698	1063	1089	3,773	3434	1684	1099	1001	186
a31	.241	7787	5683	570	575	705	1082	1092	3,750	3408	1658	1062	960	184
b32	.239	7790	5509	571	571	698	1056	1089	3,759	3426	1681	1093	995	183
a33	.240	7787	5517	570	572	698	1058	1088	3,756	3431	1683	1092	999	189
c34	.239	7803	5539	571	572	699	1062	1091	3,757	3423	1681	1098	1002	186
c35	.238	7810	5572	571	570	700	1060	1092	3,763	3452	1691	1090	995	185
d36	.169	7810	5679	564	398	698	756	1094	2,646	2415	1697	761	680	224
d37	.169	7776	5657	564	399	698	749	1089	2,607	2370	1673	745	666	222
d38	.169	7787	5682	564	398	699	750	1092	2,627	2396	1683	750	671	224
d39	.169	7777	5680	563	397	698	748	1091	2,617	2384	1678	744	668	222
d40	.169	7783	5687	563	398	698	754	1091	2,632	2397	1681	749	674	226
d41	.169	7786	5675	563	398	697	750	1092	2,621	2388	1687	749	677	227
d42	.169	7784	5612	564	398	695	746	1090	2,631	2402	1697	756	686	226

aInner ring only lighted.
 bOuter ring mostly unlighted.
 cBoth rings lighted.
 dQuestionable combustion stability.

MACA RM 585801

CONFIDENTIAL

CONFIDENTIAL

TABLE II. - Continued. PERFORMANCE OF AFTERBURNER CONFIGURATION B

(a) Concluded. Afterburning data

Engine-inlet air-flow, $w_{a,1}$, lb/sec	High pressure turbine-inlet airflow, $w_{a,4}$, lb/sec	Exhaust-nozzle inlet airflow, $w_{a,9}$, lb/sec	Engine fuel flow, $w_{f,e}$, lb/hr	Afterburner fuel flow, $w_{f,AB}$, lb/hr	Exhaust-nozzle inlet gas flow, $w_{g,9}$, lb/sec	Afterburner equivalence ratio, $\phi_{AB,ac}$	Augmented jet thrust, F_{AB} , lb	Augmented net thrust, $F_{AB,n}$, lb	Calculated afterburner total temperature, $T_{9,AB,OR}$	Exhaust-nozzle area, A_N , sq in.	Afterburner efficiency, η_{AB}	Tailpipe total-pressure loss, $\frac{P_6 - P_9}{P_6}$	Afterburner total-temperature ratio, $\frac{T_{9,AB}}{T_6}$	Run
181.95	174.47	179.44	9918	14,418	186.20	0.434	20,070	11,877	2674	980	0.758	0.110	1.559	1
180.80	173.57	178.30	9943	12,899	184.65	.388	19,981	11,772	2652	945	.820	.101	1.569	2
181.23	174.18	178.73	9770	10,865	184.46	.325	19,195	11,010	2474	943	.794	.095	1.483	3
179.59	172.88	177.11	9770	9,961	182.59	.300	18,725	10,560	2391	914	.753	.086	1.420	4
182.76	174.82	180.24	9911	8,950	185.48	.268	18,494	10,266	2271	885	.709	.083	1.350	5
142.91	137.12	140.94	7888	11,297	146.27	.437	15,362	9,371	2735	1006	.808	.107	1.645	6
138.56	132.91	136.65	7488	10,649	141.69	.412	14,636	8,841	2712	977	.816	.107	1.591	7
139.59	133.48	137.66	7463	10,264	142.58	.401	14,358	8,641	2645	981	.798	.107	1.592	8
145.20	139.62	143.20	8006	8,690	147.84	.328	14,916	8,877	2512	932	.820	.090	1.488	9
142.44	135.52	140.48	7697	7,103	144.59	.275	13,690	7,905	2306	907	.735	.083	1.378	10
143.98	138.73	142.00	7862	5,486	145.71	.206	13,315	7,400	2084	823	.602	.074	1.235	11
144.43	139.49	142.44	7877	4,637	145.92	.173	12,937	7,038	1979	805	.538	.074	1.176	12
144.34	139.61	142.35	7891	3,636	145.55	.136	12,520	6,618	1867	773	.412	.071	1.108	13
101.60	97.94	100.20	5670	8,698	104.19	.471	11,259	6,613	2645	981	.669	.103	1.566	14
100.76	96.81	99.37	5699	7,484	103.03	.412	10,756	6,323	2557	941	.682	.089	1.504	15
100.93	97.52	99.53	5706	6,073	102.80	.330	10,431	5,951	2392	893	.679	.082	1.407	16
100.74	97.62	99.35	5663	4,601	102.20	.252	9,927	5,441	2195	856	.631	.081	1.295	17
100.66	97.65	98.27	5699	2,934	101.67	.163	9,382	4,883	1976	771	.521	.072	1.160	18
80.70	78.24	78.59	4345	5,872	82.45	.392	7,421	4,741	2553	1005	.737	.102	1.533	19
80.58	78.25	78.47	4406	4,403	81.92	.297	6,957	4,326	2278	929	.653	.090	1.364	20
80.68	78.20	78.57	4313	3,208	81.66	.216	6,554	3,902	2058	876	.569	.091	1.246	21
81.73	78.91	80.60	4464	2,160	82.44	.147	6,407	3,725	1913	825	.524	.090	1.150	22
81.46	78.78	80.33	4388	2,038	82.14	.136	6,273	3,606	1845	801	.412	.083	1.111	23
64.98	62.51	64.08	3586	7,992	67.30	.673	6,739	3,940	2449	971	.373	.108	1.466	a24
65.49	63.59	64.59	3614	7,373	67.64	.613	6,944	4,005	2460	977	.413	.109	1.462	a25
64.87	62.53	63.98	3550	6,570	66.79	.549	6,569	3,801	2381	935	.408	.099	1.414	a26
65.20	63.26	64.30	3722	5,929	66.98	.499	6,906	4,000	2476	927	.493	.096	1.435	b27
65.29	62.58	64.39	3665	5,670	66.98	.482	6,411	3,623	2239	921	.367	.092	1.332	a28
64.94	62.98	64.04	3532	4,612	66.30	.387	5,987	3,228	2045	885	.310	.098	1.236	a29
65.15	62.87	64.25	3661	4,453	66.48	.379	6,175	3,415	2131	874	.372	.089	1.265	a30
64.91	63.05	64.02	3427	3,366	65.91	.274	5,718	2,954	1889	843	.259	.096	1.139	a31
64.83	62.85	63.94	3618	3,265	65.85	.279	6,123	3,364	2133	876	.509	.090	1.269	b32
64.69	62.57	63.80	3647	3,031	65.66	.262	5,848	3,123	1977	837	.348	.086	1.175	a33
65.03	62.99	64.13	3658	2,448	65.83	.214	6,049	3,296	2091	857	.603	.088	1.237	c34
65.07	62.83	64.17	3643	2,002	65.74	.171	5,916	3,158	2008	844	.567	.087	1.187	c35
45.50	44.10	44.87	2599	8,010	47.82	.967	3,892	2,459	2174	948	.151	.106	1.281	d36
44.83	43.55	44.21	2509	7,092	46.88	.865	3,839	2,412	2218	952	.199	.105	1.326	d37
45.23	43.91	44.61	2527	5,908	46.95	.713	3,817	2,395	2195	940	.229	.105	1.304	d38
44.79	43.47	44.17	2466	4,907	46.22	.594	3,681	2,266	2106	936	.224	.102	1.255	d39
45.21	43.88	44.58	2549	4,140	46.44	.422	3,654	2,244	2096	904	.310	.100	1.247	d40
45.21	43.87	44.58	2520	3,348	46.21	.403	3,639	2,230	2071	892	.303	.097	1.228	d41
45.19	43.88	44.56	2538	2,329	45.91	.282	3,623	2,210	2059	860	.401	.093	1.213	d42

^aInner ring only lighted.^bOuter ring mostly unlighted.^cBoth rings lighted.^dQuestionable combustion stability.

TABLE II. - Continued. PERFORMANCE OF AFTERBURNER CONFIGURATION B

(b) Nonafterburning data

Run	Engine-inlet Reynolds number index, ReI	High-pressure compressor rotor speed, N_{HP} , rpm	Low-pressure compressor rotor speed, N_{LP} , rpm	Engine-inlet total temperature, T_1 , $^{\circ}R$	Engine-inlet total pressure, P_1 , lb/sq ft abs	High-pressure compressor-inlet total temperature, T_2 , $^{\circ}R$	High-pressure compressor-inlet total pressure, P_2 , lb/sq ft abs	High-pressure compressor-outlet total temperature, T_3 , $^{\circ}R$	High-pressure compressor-outlet total pressure, P_3 , lb/sq ft abs	High-pressure turbine-inlet total pressure, P_4 , lb/sq ft abs	Low-pressure turbine-outlet total pressure, P_6 , lb/sq ft abs	Exhaust nozzle-inlet total temperature, T_9 , $^{\circ}R$	Exhaust nozzle-inlet total pressure, P_9 , lb/sq ft abs	Tank static pressure, P_{tank} , lb/sq ft abs
1	0.641	7793	5365	570	1529	688	2829	1078	-----	-----	3124	1684	2916	424
2	.515	7790	5403	573	1238	694	2282	1084	8254	7526	2470	1672	2296	450
3	.425	6950	4880	436	716	532	1360	851	5080	4646	1494	1333	1389	415
4	.365	7768	5401	572	875	692	1615	1080	5832	5316	1743	1678	1622	246
5	.293	7806	5570	573	705	701	1307	1096	4662	4255	1356	1668	1252	380
6	.239	7784	5539	574	575	701	1066	1091	3757	3412	1092	1678	1008	184
7	.238	7810	5510	570	569	703	1070	1088	3777	3441	1084	1681	997	165
8	.168	7816	5711	566	396	702	753	1097	2652	2418	758	1695	695	209
9	.381	7784	5242	699	1174	816	1899	1192	5791	5204	1728	1678	1614	379
10	.379	7604	5148	696	1162	807	1843	1167	5330	4777	1575	1592	1464	411
11	.383	7420	4997	696	1174	802	1810	1140	4982	4443	1454	1500	1354	396
12	.379	7210	4823	696	1163	794	1747	1114	4538	4026	1312	1405	1218	391
13	.375	7000	4685	696	1150	791	1672	1090	4093	3606	1175	1302	1093	358
14	.382	6977	4630	696	1171	787	1698	1079	4139	3641	1190	1282	1108	366
15	.403	7580	5035	758	1371	867	2060	1217	5478	4880	1625	1564	1517	389
16	.386	7600	5054	784	1370	893	2029	1249	5299	4714	1584	1591	1482	392
17	.375	7625	5051	806	1375	907	2030	1252	5243	4663	1561	1582	1460	381

TABLE II. - Concluded. PERFORMANCE OF AFTERBURNER CONFIGURATION B

(b) Concluded. Nonafterburning data

Engine-inlet air-flow, $w_{a,1}$, lb/sec	High-pressure turbine-inlet airflow, $w_{a,4}$, lb/sec	Exhaust-nozzle inlet airflow, $w_{a,9}$, lb/sec	Engine fuel flow, $w_{f,e}$, lb/hr	Exhaust-nozzle inlet gas flow, $w_{g,9}$, lb/sec	Unaugmented jet thrust, F_J , lb	Unaugmented net thrust, $F_{J,N}$, lb	Calculated engine jet thrust, F_J , lb	Exhaust-nozzle velocity coefficient, C_{ve}	Exhaust-nozzle area, A_N , sq in.	Tailpipe total-pressure loss, $\frac{P_6 - P_9}{P_6}$	Run
181.04	176.04	178.54	9961	181.31	15,552	10,708	15,852	0.975	723	0.067	1
143.74	136.15	141.76	7837	143.94	11,702	5,850	11,977	.977	736	.071	2
99.99	96.57	98.61	4298	99.80	6,446	3,748	6,673	.966	738	.070	3
101.32	96.82	99.92	5652	101.49	8,463	3,969	8,810	.961	725	.070	4
80.61	77.67	79.50	4428	80.73	5,879	3,236	6,032	.975	758	.076	5
64.65	61.67	63.76	3590	64.76	5,304	2,542	5,468	.970	749	.076	6
65.33	63.13	64.43	3640	65.44	5,431	2,564	5,612	.968	739	.081	7
45.10	43.71	44.47	2569	45.18	3,298	1,804	3,412	.967	766	.084	8
98.91	94.53	97.55	4892	98.91	7,828	3,180	7,939	.986	720	.066	9
93.51	90.03	92.22	4162	93.38	6,770	2,527	6,965	.972	727	.070	10
89.49	86.20	88.26	3571	89.25	6,209	2,078	6,380	.973	719	.069	11
83.94	80.96	82.78	2912	83.59	5,435	1,555	5,610	.969	723	.071	12
77.57	74.80	76.50	2354	77.15	4,863	1,182	4,944	.984	742	.069	13
78.93	75.95	77.84	2311	78.48	4,876	1,134	4,976	.980	724	.070	14
96.36	92.38	95.03	3942	96.13	7,101	2,187	7,286	.975	722	.066	15
92.05	88.75	90.78	3766	91.83	6,790	2,029	6,962	.975	722	.065	16
90.64	87.53	89.39	3686	90.41	6,737	1,939	6,861	.982	721	.065	17

CONFIDENTIAL

CONFIDENTIAL

NACA RM 5858G01

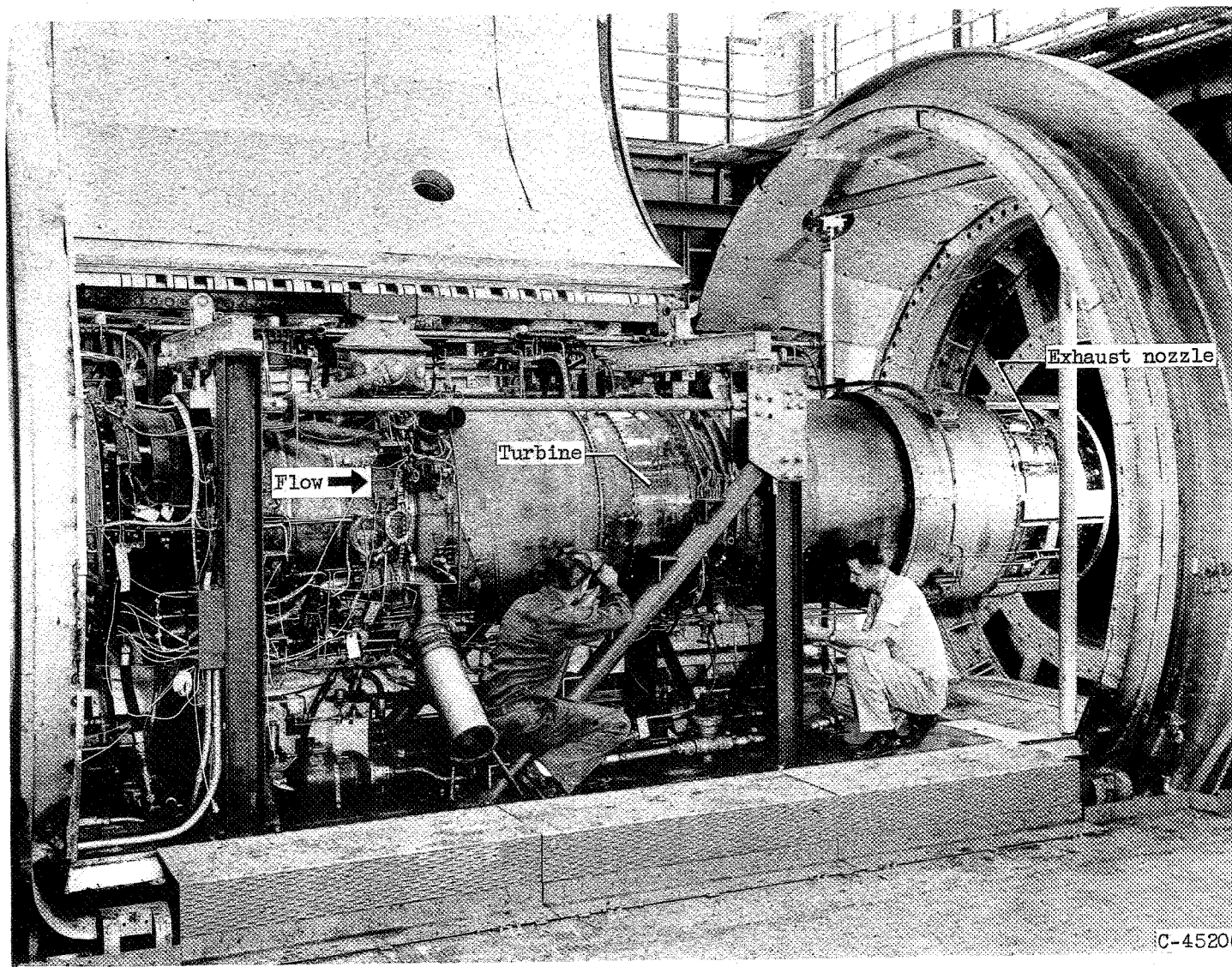


Figure 1. - Iroquois turbojet engine and afterburner installed in altitude test chamber.

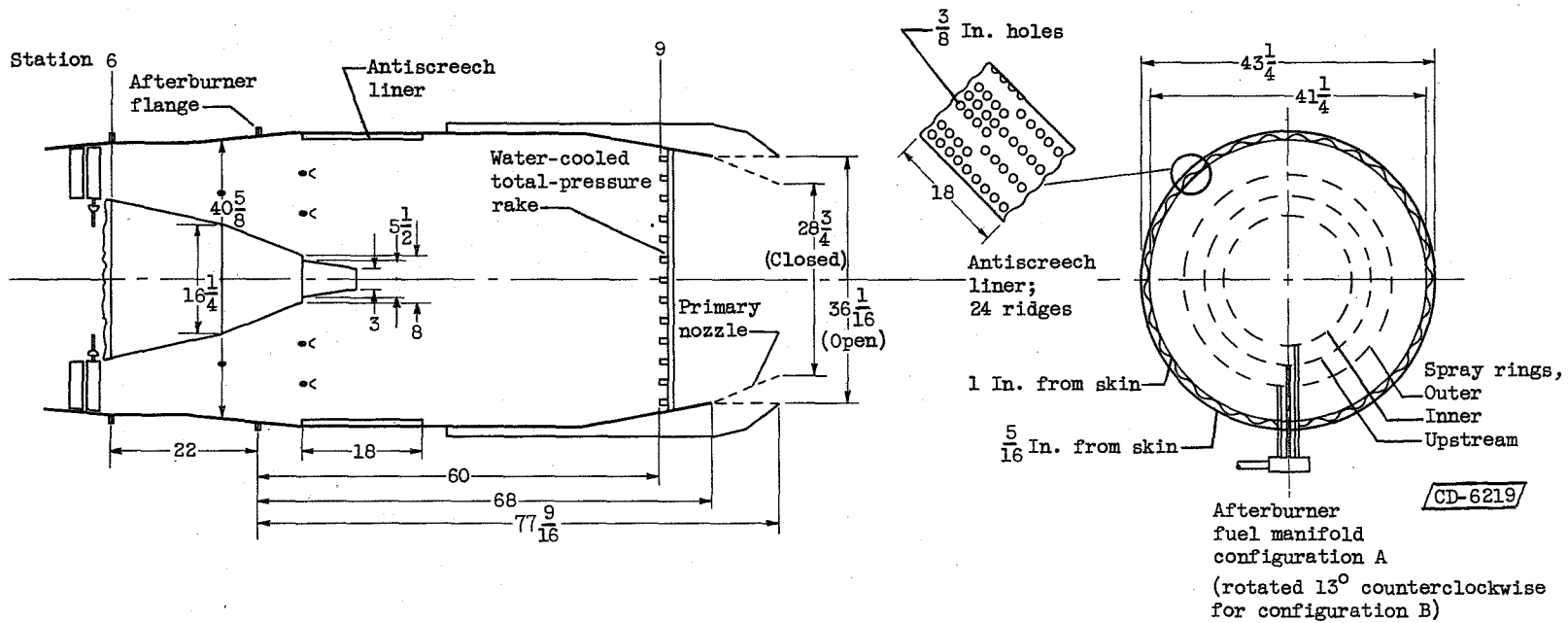
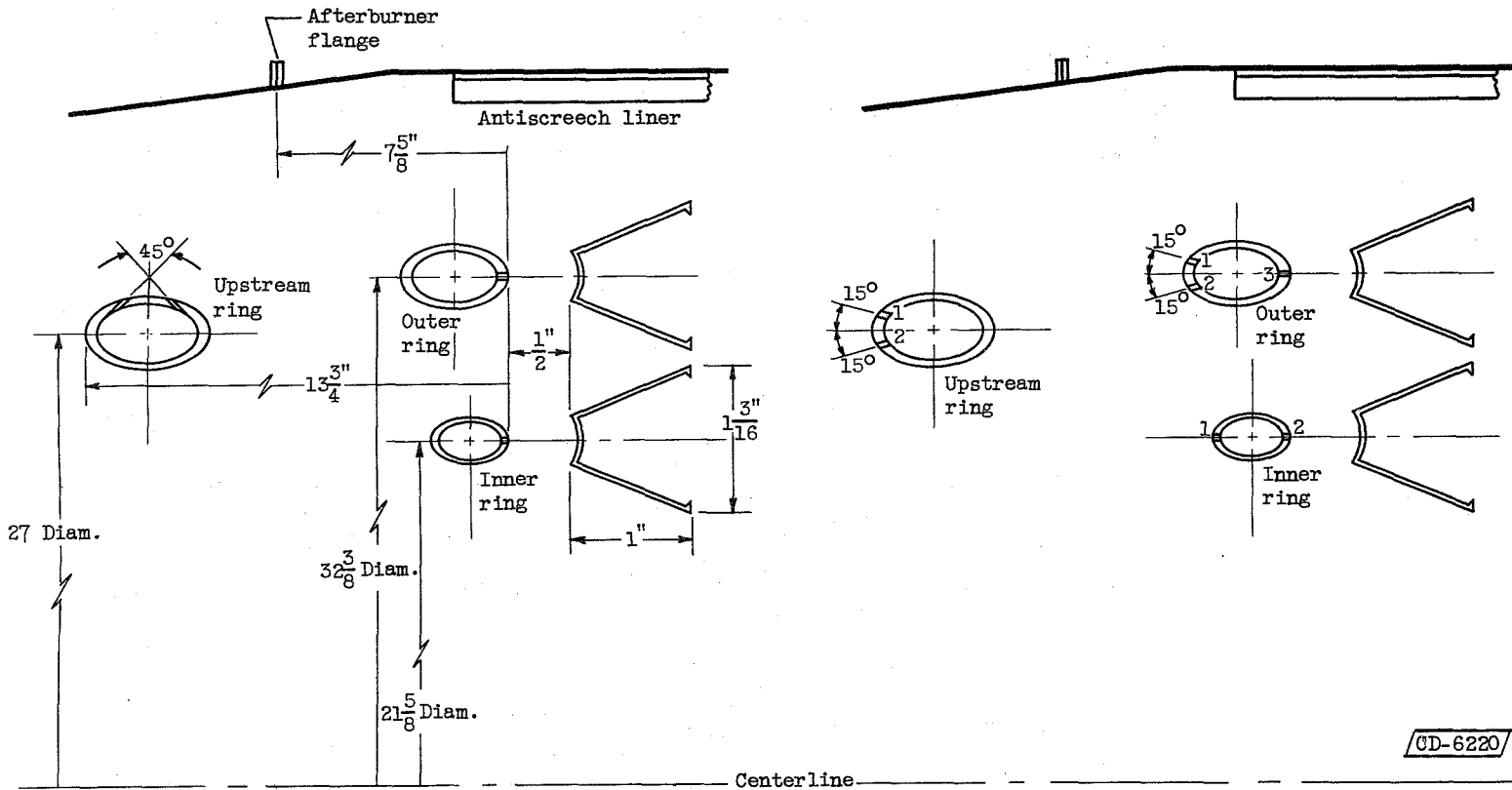


Figure 2. - Schematic diagram of basic afterburner showing location of various components. (All dimensions in inches.)



CD-6220

CONFIGURATION A

CONFIGURATION B

Ring	Tube diameter, in.	Wall thickness, in.	Number of orifices	Orifice diameter, in.	Fuel flow, percent
Upstream	1	0.095	138(69 pr)	0.024-0.025	45.3
Outer	7/8	.095	70	.032-.034	41.0
Inner	5/8	.072	60	.020-.021	13.7

Ring	Tube diameter, in.	Wall thickness, in.	Orifice	Number of orifices	Orifice diameter, in.	Fuel flow percent
Upstream	1	0.095	1	70	0.027-0.028	26.6
			2	35	.031-.032	17.6
Outer	7/8	.095	1	35	.023-.024	9.7
			2	35	.023-.024	9.7
			3	70	.024-.025	21.8
Inner	5/8	.072	1	40	.018-.019	6.5
			2	40	.020-.021	8.1

Figure 3. - Schematic diagram showing differences in fuel injector rings for configurations A and B.

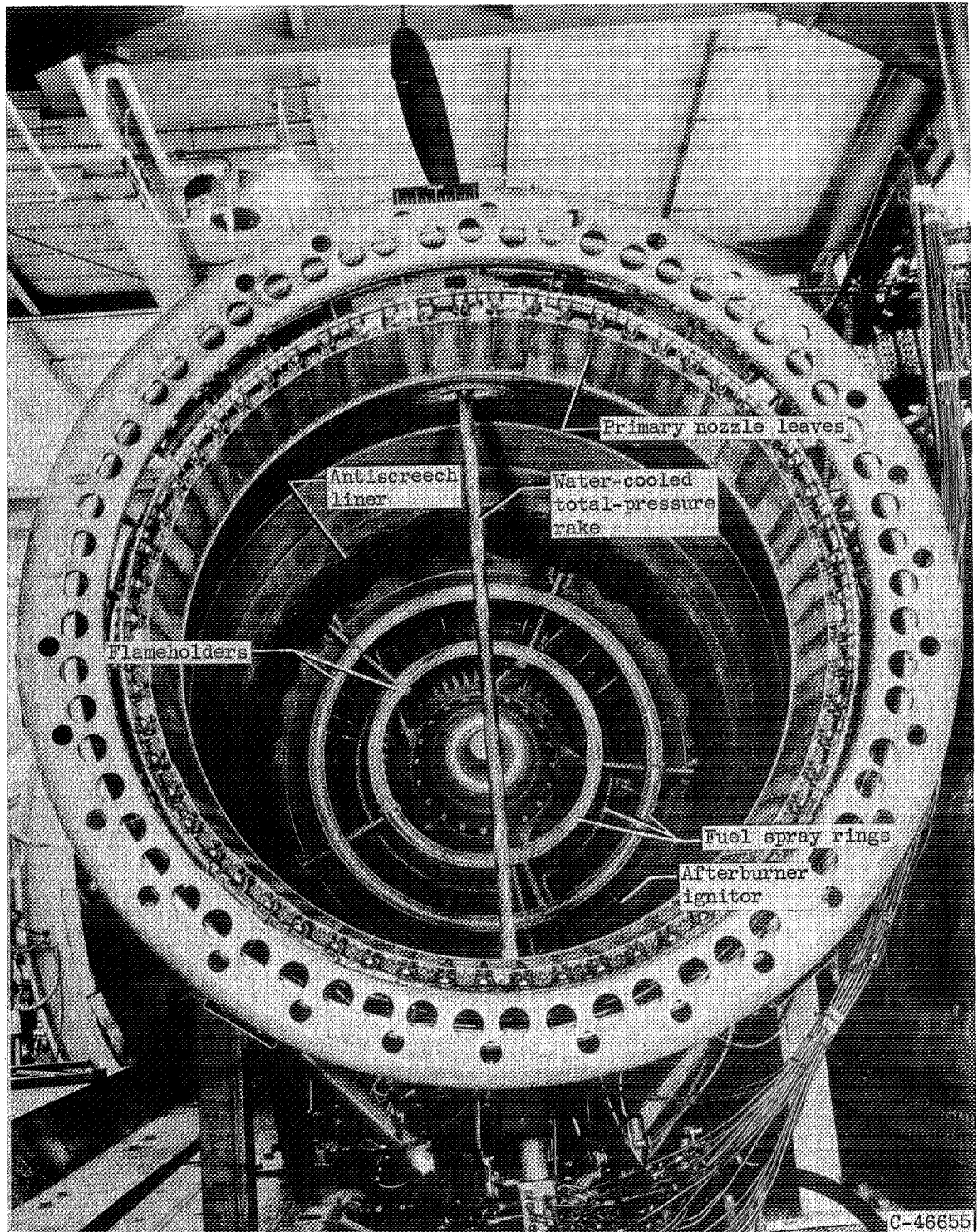
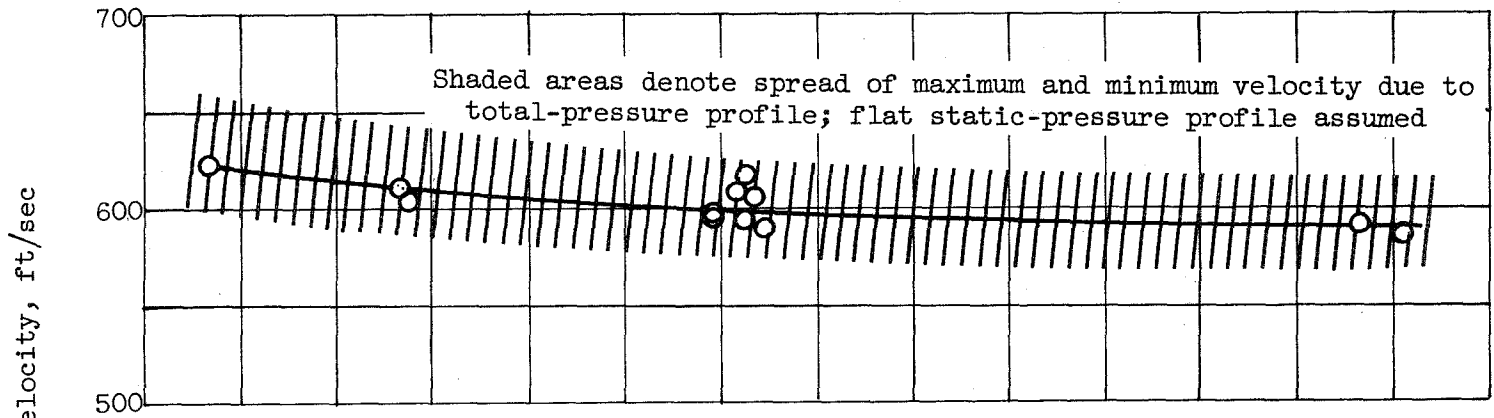
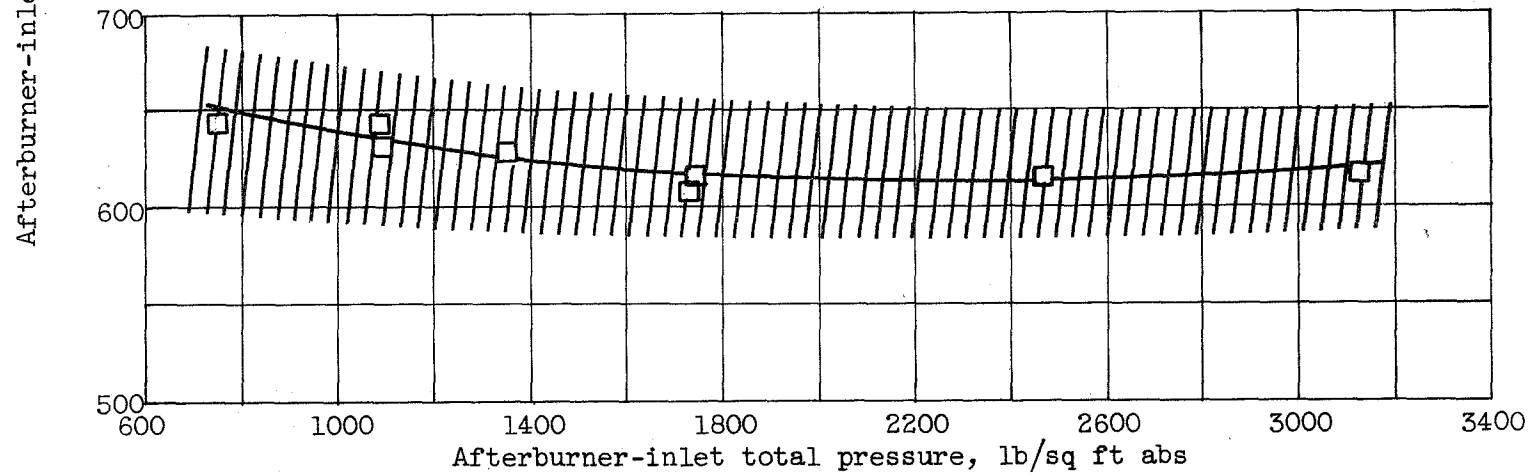


Figure 4. - Iroquois afterburner looking upstream.



(a) Configuration A.



(b) Configuration B.

Figure 5. - Afterburner-inlet velocity over pressure range investigated. Engines at rated conditions; nonafterburning data.

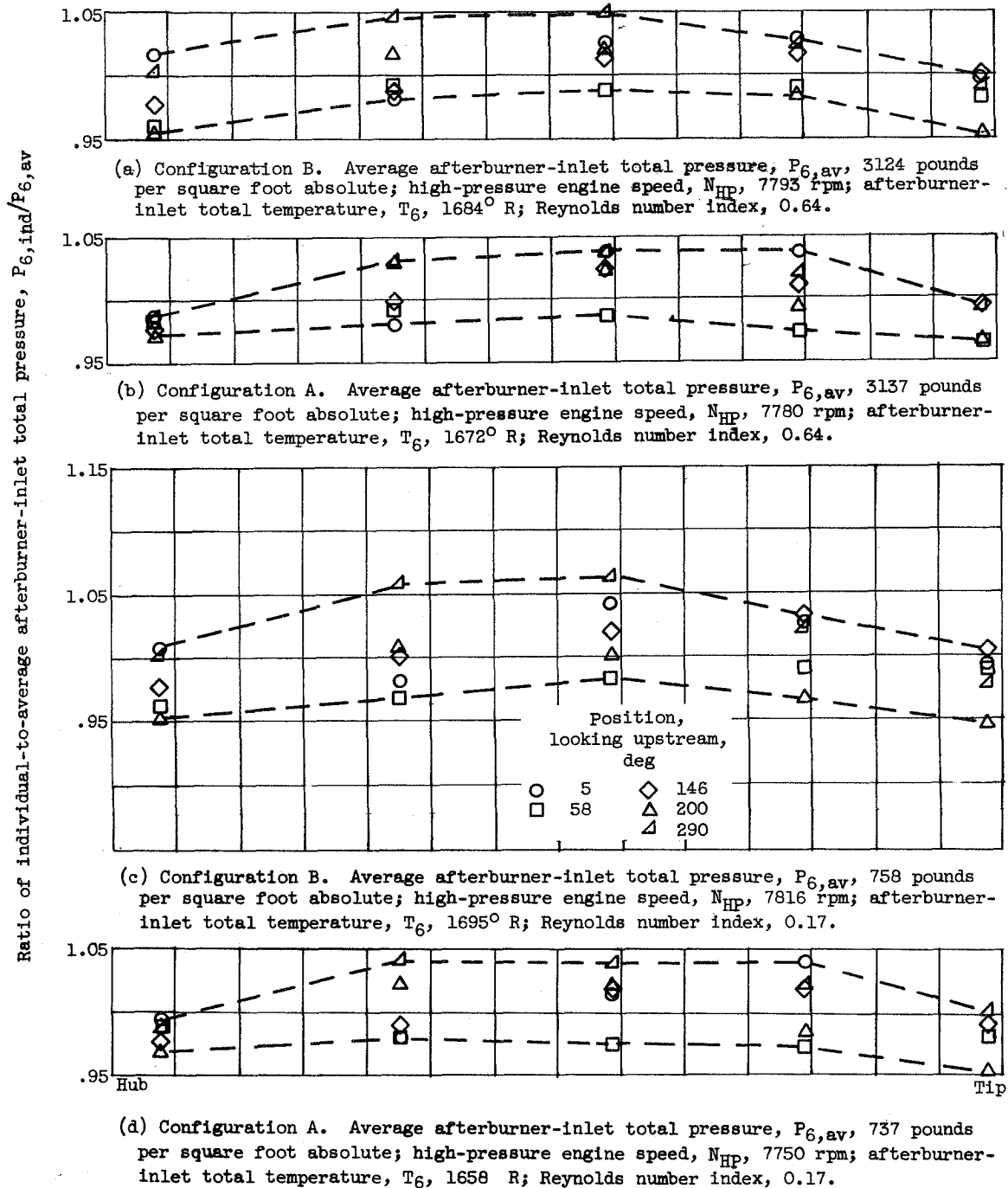
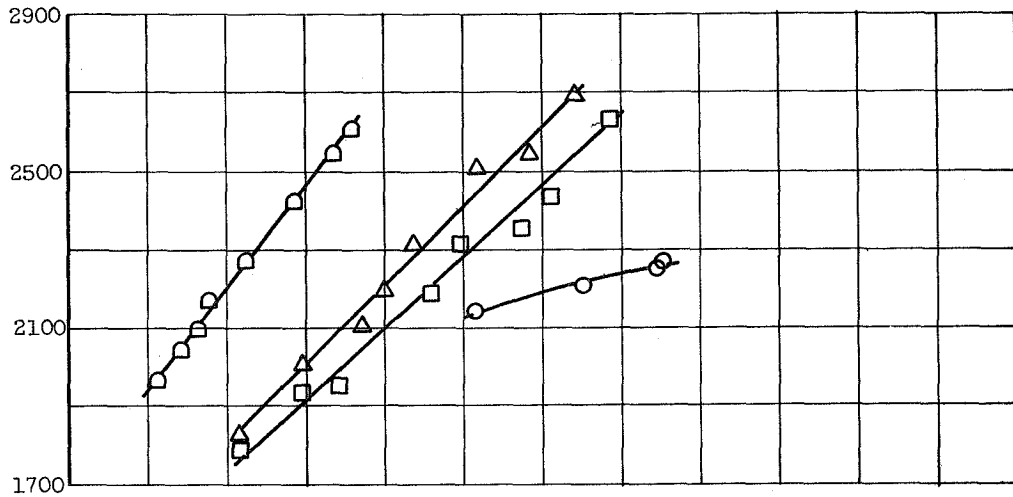
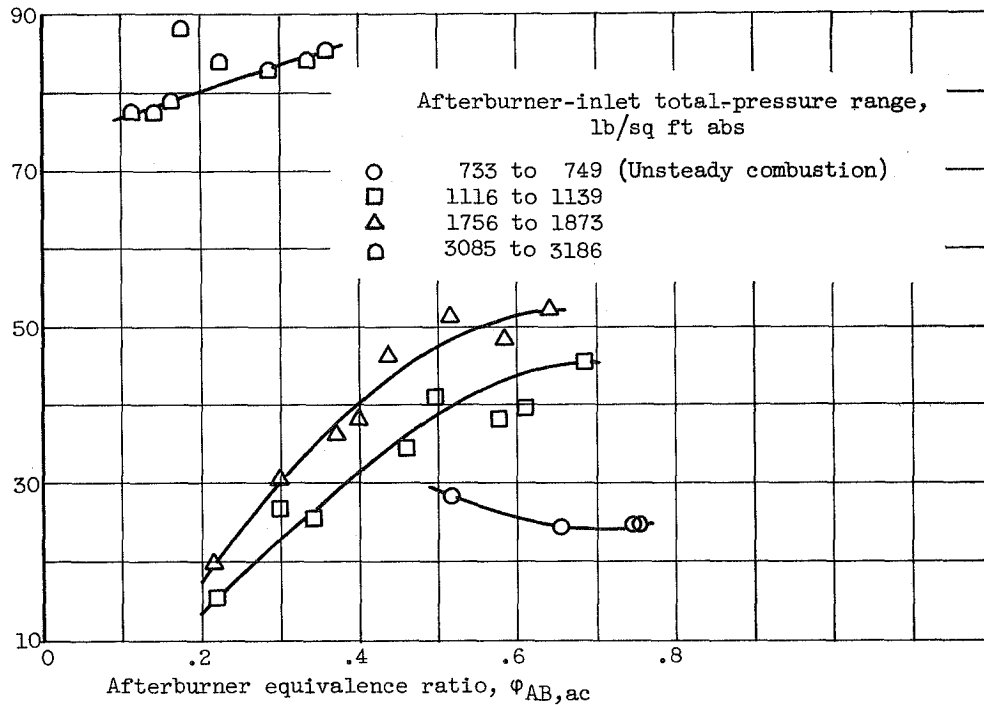


Figure 6. - Afterburner-inlet total-pressure profiles (station 6). Nonafterburning data.

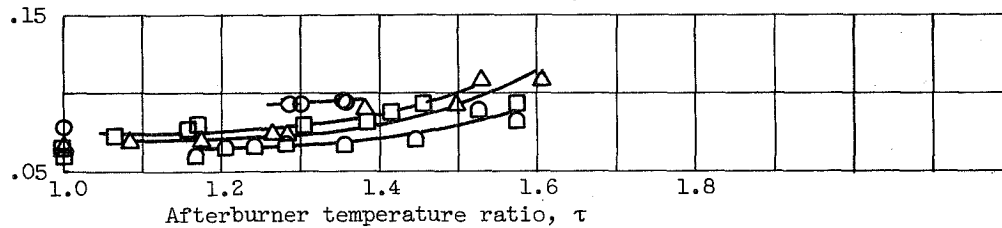
Afterburner combustion temperature, T_9 , C_R



Afterburner combustion efficiency, η_{AB} , percent

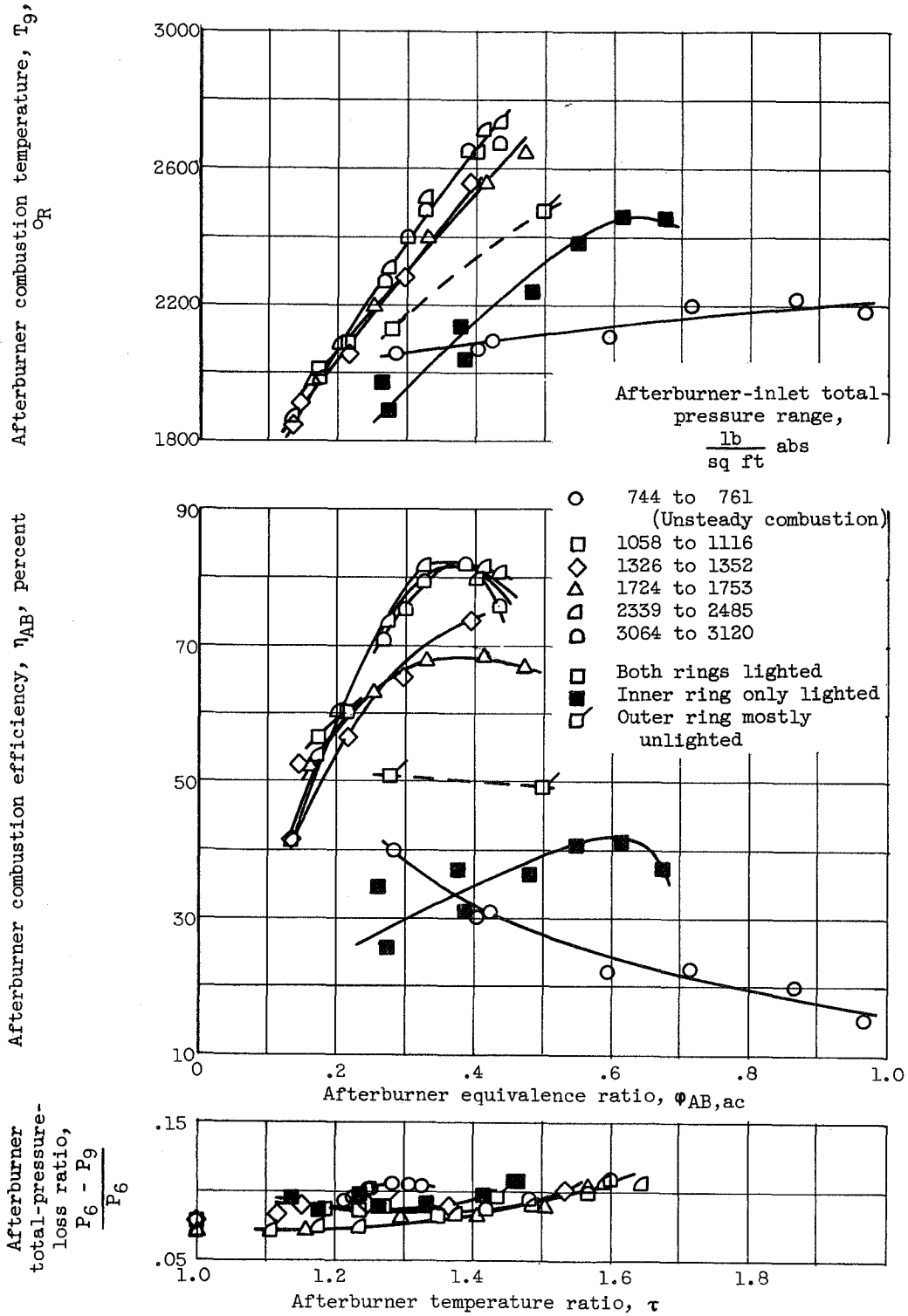


Afterburner total-pressure-loss ratio, $\frac{P_6 - P_9}{P_6}$



(a) Configuration A.

Figure 7. - Combustion performance of afterburner over a range of afterburner-inlet total pressures.



(b) Configuration B.

Figure 7. - Concluded. Combustion performance of afterburner over a range of afterburner-inlet total pressures.

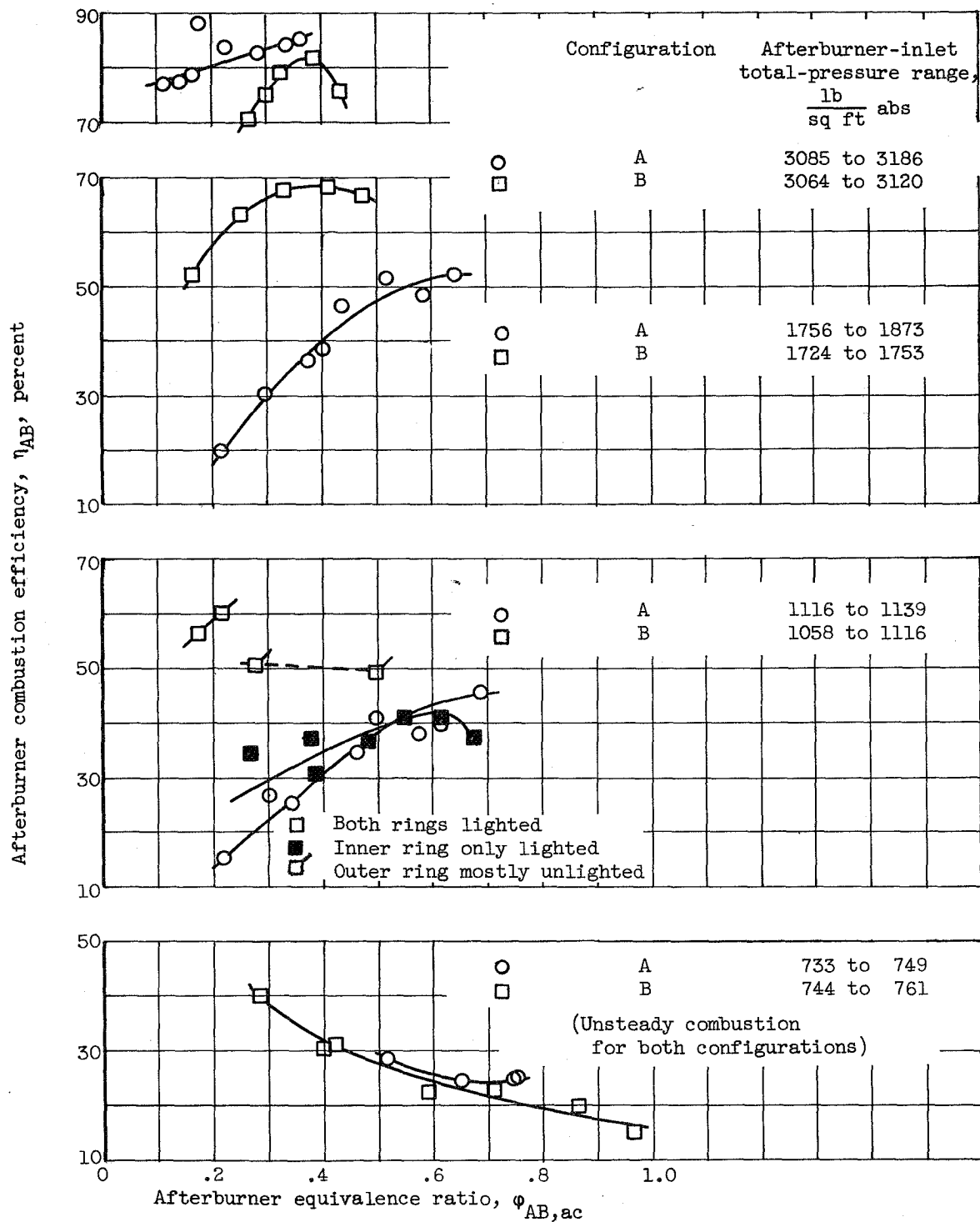


Figure 8. - Comparison of combustion efficiencies for afterburner configurations A and B.

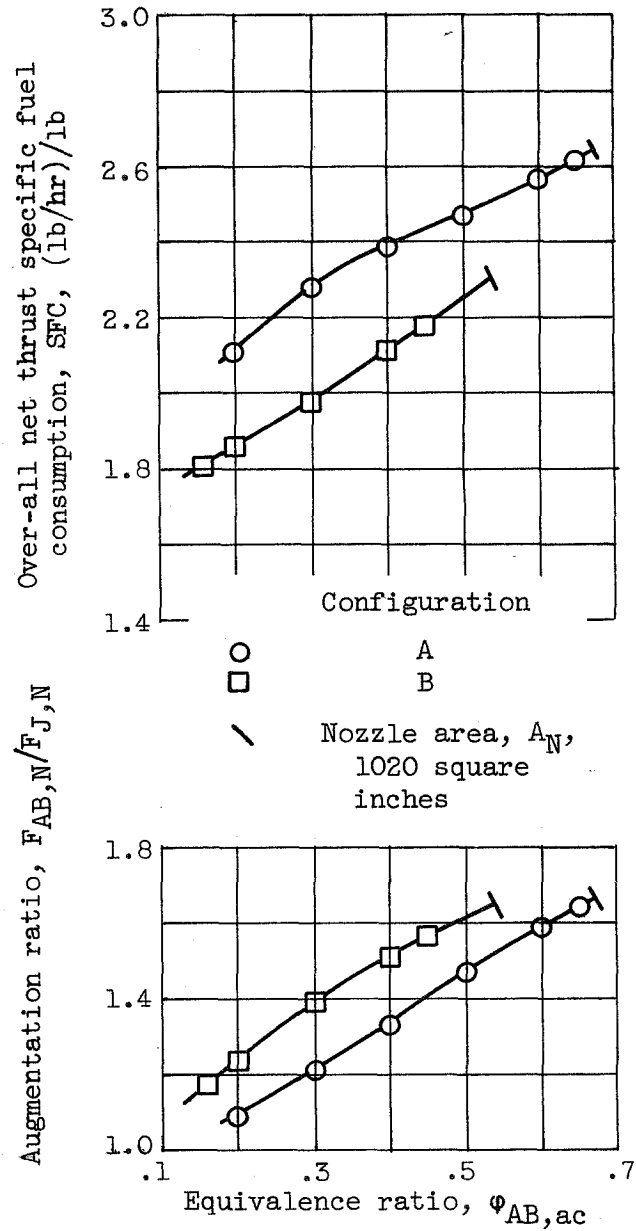


Figure 9. - Calculated performance for configurations A and B. Altitude, 50,400 feet; flight Mach number, 1.5.

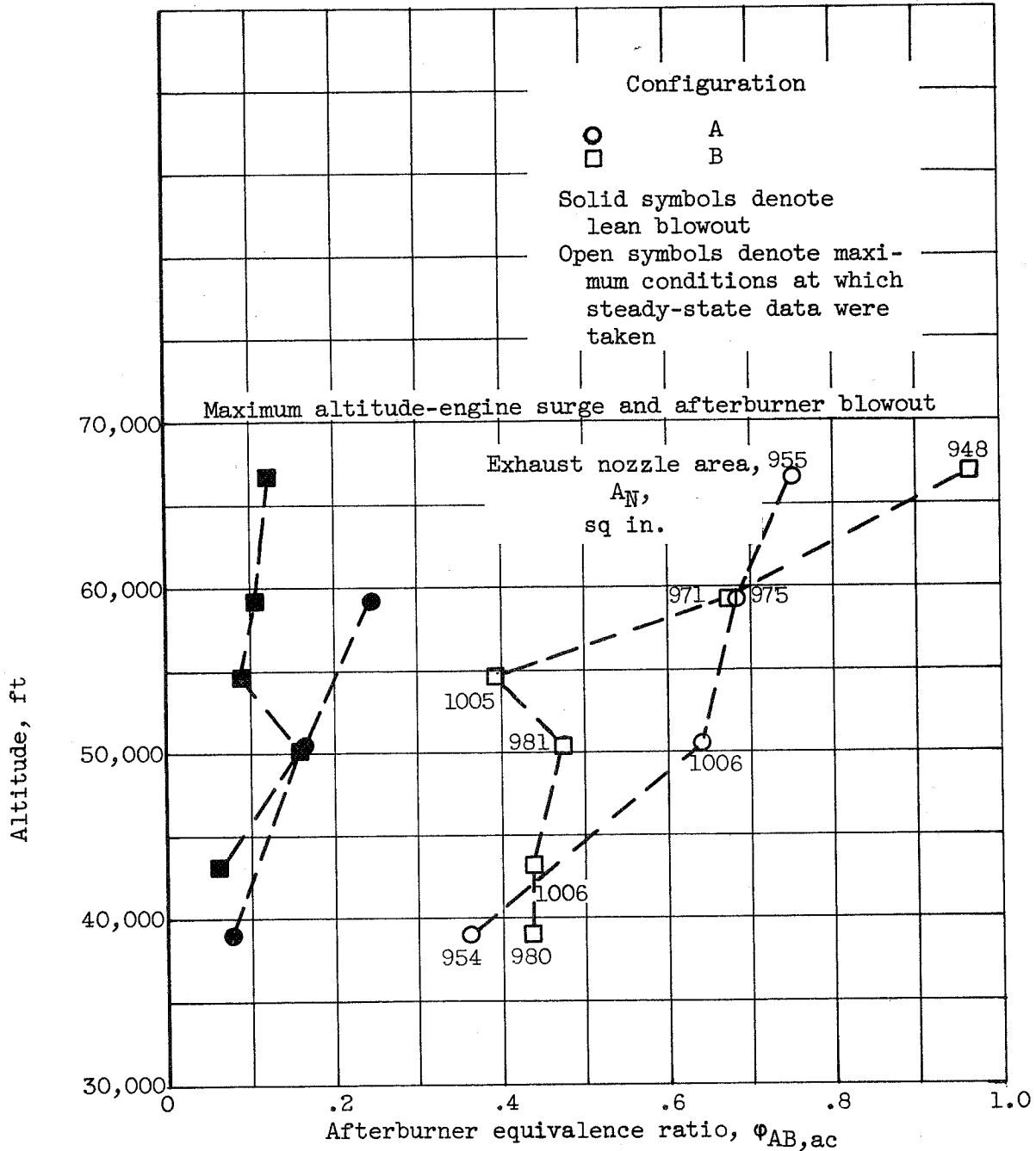


Figure 10. - Afterburner operational limits. Configurations A and B; flight Mach number, 1.5.

ALTITUDE PERFORMANCE OF THE AFTERBURNER ON THE
IROQUOIS TURBOJET ENGINE

COORD. NO. AF-P-6

By Donald E. Groesbeck and Daniel J. Peters

ABSTRACT

The performance and operational characteristics of two afterburner configurations for the Iroquois turbojet engine were evaluated over a range of afterburner equivalence ratios at afterburner-inlet pressures from 733 to 3186 pounds per square foot absolute. At a flight Mach number of 1.5, these pressures correspond to an altitude range of 38,700 to 66,800 feet. Peak efficiencies of 0.80 to 0.85 for both configurations were reached at an afterburner-inlet pressure of approximately 3100 pounds per square foot absolute and at equivalence ratios of 0.35 to 0.40. Reduction in afterburner-inlet pressure severely affected combustion efficiency.

INDEX HEADING

Turbines, Gas - Afterburning

3.3.2.2

NACA RM E58G01

Restriction/Classification
Cancelled ~~CONFIDENTIAL~~

ALTITUDE PERFORMANCE OF THE AFTERBURNER ON THE
IROQUOIS TURBOJET ENGINE

Donald E. Groesbeck

Donald E. Groesbeck

Daniel J. Peters

Daniel J. Peters

Approved:

Bruce T. Lundin

Bruce T. Lundin
Chief
Propulsion Systems Division

sks-7/7/58

Restriction/Classification
Cancelled

~~CONFIDENTIAL~~

NACA-CLEVELAND, OHIO